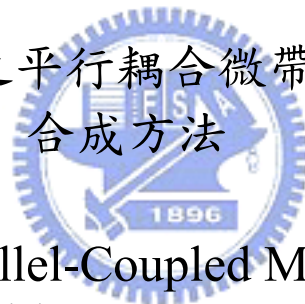


國立交通大學

電信工程學系

博士論文

具精確頻寬之平行耦合微帶線帶通濾波器
合成方法



Synthesis of Parallel-Coupled Microstrip Bandpass
Filters with Accurate Bandwidths

研究生：金國生

(Kuo-Sheng Chin)

指導教授：郭仁財 博士

(Dr. Jen-Tsai Kuo)

中華民國九十四年七月

具精確頻寬之平行耦合微帶線帶通濾波器
合成方法

Synthesis of Parallel-Coupled Microstrip
Bandpass Filters with Accurate Bandwidths

研究生: 金國生 (Kuo-Sheng Chin)

指導教授: 郭仁財 博士 (Dr. Jen-Tsai Kuo)



A Dissertation Submitted to
Department of Communication Engineering
College of Engineering
National Chiao Tung University
in Partial Fulfillment of the Requirements
in
Communication Engineering
July 2005
Hsinchu, Taiwan, Republic of China

中華民國九十四年七月

推 薦 函

中華民國九十四年六月二十七日

一、事由：本校電信研究所博士班研究生 金國生 提出論文以參加國立交通大學
博士班論文口試。

二、說明：本校電信研究所博士班研究生 金國生 已完成本校電信研究所規定之
學科課程及論文研究之訓練。

有關學科部分，金君已修滿十八學分之規定（請查閱學籍資料）並通過資
格考試。

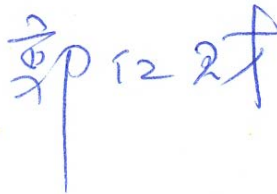
有關論文部分，金君已完成其論文初稿，相關之論文亦分別發表或即將發
表於國際期刊（請查閱附件）並滿足論文計點之要求。

總而言之，金君已具備國立交通大學電信研究所應有之教育及訓練水準，

因此特推薦

金君參加國立交通大學電信工程學系博士班論文口試。

交通大學電信工程學系教授 郭仁財



國立交通大學

論文口試委員審定書

本校 電信工程 學系博士班 金國生 君

所提論文 具精確頻寬之平行耦合微帶線帶通濾波器合成方法
Synthesis of Parallel-Coupled Microstrip Bandpass Filters with
Accurate Bandwidths

合於博士資格水準、業經本委員會評審認可。

口試委員：

郭仁財

趙孝承

吳瑞光

陳俊明

沈世榮

張志揚

姚聖芳

孫毅文

施廷直

指導教授：

郭仁財

系主任：

唐震寰

教授

中華民國九十四年七月十四日

Department of Communication Engineering
National Chiao Tung University
Hsinchu, Taiwan, R.O.C.

Date: July 14, 2005

We have carefully read the dissertation entitled

Synthesis of Parallel-Coupled Microstrip Bandpass
Filters with Accurate Bandwidths

submitted by Kuo-Sheng Chin in partial
fulfillment of the requirements of the degree of DOCTOR OF
PHILOSOPHY and recommend its acceptance.

Jen-Tsai Kuo

Hsi-Yung Chao

Shih-Der Wu

Chun-Hsiung Chen

Shih-Je Chen

Chi-Yang Chung

Sheng-Fuh Chang

Chih-Jen Hsu

Eric Shin

Thesis Advisor:

Jen-Tsai Kuo

Chairman

Jenn-Hwan Tseng

Department of Communication Engineering:

國立交通大學

博碩士論文全文電子檔著作權授權書

(提供授權人裝訂於紙本論文書名頁之次頁用)

本授權書所授權之學位論文，為本人於國立交通大學 電信工程 系所
電波組 組，93 學年度第 2 學期取得博士學位之論文。

論文題目：具精確頻寬之平行耦合微帶線帶通濾波器合成方法

指導教授：郭仁財

同意 不同意

本人茲將本著作，以非專屬、無償授權國立交通大學與台灣聯合大學系統圖書館：基於推動讀者間「資源共享、互惠合作」之理念，與回饋社會與學術研究之目的，國立交通大學及台灣聯合大學系統圖書館得不限地域、時間與次數，以紙本、光碟或數位化等各種方法收錄、重製與利用；於著作權法合理使用範圍內，讀者得進行線上檢索、閱覽、下載或列印。

論文全文上載網路公開之範圍及時間：

本校及台灣聯合大學系統區域網路	<input checked="" type="checkbox"/> 中華民國 94 年 7 月 14 日公開
校外網際網路	<input checked="" type="checkbox"/> 中華民國 94 年 7 月 14 日公開

授權人：金國生

親筆簽名：金國生

中華民國 94 年 7 月 14 日

國立交通大學

博碩士紙本論文著作權授權書

(提供授權人裝訂於全文電子檔授權書之次頁用)

本授權書所授權之學位論文，為本人於國立交通大學 電信工程 系所
電波組 組，93 學年度第 2 學期取得博士學位之論文。

論文題目：具精確頻寬之平行耦合微帶線帶通濾波器合成方法

指導教授：郭仁財

■ 同意

本人茲將本著作，以非專屬、無償授權國立交通大學，基於推動讀者間「資源共享、互惠合作」之理念，與回饋社會與學術研究之目的，國立交通大學圖書館得以紙本收錄、重製與利用；於著作權法合理使用範圍內，讀者得進行閱覽或列印。

本論文為本人向經濟部智慧局申請專利(未申請者本條款請不予理會)的附件之一，申請文號為：_____，請將論文延至____年____月____日再公開。

授權人：金國生

親筆簽名：金國生

中華民國 94 年 7 月 14 日

國家圖書館博碩士論文電子檔案上網授權書

ID:GT009013806

本授權書所授權之學位論文，為本人於國立交通大學電信工程系所
電波組組，93學年度第2學期取得博士學位之論文。

論文題目：具精確頻寬之平行耦合微帶線帶通濾波器合成方法

指導教授：郭仁財

茲同意將授權人擁有著作權之上列論文全文（含摘要），非專屬、無償授權國家圖書館，不限地域、時間與次數，以微縮、光碟或其他各種數位化方式將上列論文重製，並得將數位化之上列論文及論文電子檔以上載網路方式，提供讀者基於個人非營利性質之線上檢索、閱覽、下載或列印。

※ 讀者基於非營利性質之線上檢索、閱覽、下載或列印上列論文，應依著作權法相關規定辦理。

授權人：金國生

親筆簽名：金國生

中華民國 94 年 7 月 14 日


具精確頻寬之平行耦合微帶線帶通濾波器合成方法

研究生: 金國生

指導教授: 郭仁財 博士

國立交通大學 電信工程學系

摘要



在本論文，作者提出平行耦合微帶線帶通濾波器之新合成方法，可獲取精確頻寬。傳統上，一段平行線耦合級係以兩段 $1/4$ 波長傳輸線及中間夾一個導納轉換器來等效，由於導納轉換器並不具隨頻率改變之特性，因此此種等效模式僅在設計小頻寬時較為準確，當設計較大頻寬時，實際頻寬會明顯大幅縮減。為改善此問題，論文第一部份提出以頻帶邊緣等效取代中心頻率等效之觀念來修正傳統公式，以獲取較為精確之頻寬。更進一步地，論文第二部份提出以介入損耗函數來合成具有精確頻寬之平行耦合線帶通濾波器之方法。介入損耗函數可直接由耦合級串接之 $ABCD$ 矩陣推導得出，而不需使用含導納轉換器之等效電路，藉由與最大平坦函數及柴比雪夫函數比對係數，得出所需之合成公式。由於在某些嚴苛設計規格下，耦合線線寬及線距可能過窄難以實現，此時可運用合成公式提供之自由度適當選擇解答，放寬中間耦合級之尺寸，將困難移至兩端(輸入及輸出端)耦合級，並採用擇定饋入法(Tapped input)方式來實現端級。作者並實際合成數組大頻寬濾波器作為範例，以模擬及量測數據來與本文之理論計算結果做比較，證實此方法可行且頻寬相當精確。

Synthesis of Parallel-Coupled Microstrip Bandpass Filters with Accurate Bandwidths

Student: Kuo-Sheng Chin

Advisor: Dr. Jen-Tsai Kuo

Department of Communication Engineering
National Chiao Tung University

Abstract

In the thesis, authors propose the new synthesis methods of parallel-coupled microstrip bandpass filters (PCBPFs) with accurate bandwidth. In a conventional design, the equivalence of a coupled stage is established by using two quarter-wave transmission line sections with a J -inverter in between. Since the J -inverter is independent of frequency, the conventional equations are accurate only for filters with relatively narrow bandwidths. When a large bandwidth is designed, filters synthesized based on the conventional method will have a fractional bandwidth less than specification. In the first part of the dissertation, for recovering the bandwidth decrement, the correction $\theta = (\pi/2)(1 \pm \Delta/2)$ is incorporated into the synthesis formulas to modify the conventional method. Furthermore, the insertion loss (IL) functions are derived for synthesis of PCBPFs with accurate bandwidth. The synthesis is based on the composite $ABCD$ matrix of all coupled stages instead of modeling each stage with the J -inverter equivalent circuit. Synthesis equations are established by matching the coefficients of IL function with the maximally-flat and Chebyshev functions. The under-determined conditions leave several degrees of freedom in choosing the circuit dimensions. By properly utilizing these degrees of freedom, the problem resulted from the tight coupled-line dimensions can be resolved by gathering all difficulties to the end stages and employing tapped input/output to replace the end stages. Several filters are simulated, fabricated and measured to demonstrate the formulation and circuit synthesis. The measured results manifest very accurate bandwidths.

謝誌

「你或向左、或向右，你必聽見後邊有聲音說，這是正路，要行在其間。」

—以賽亞書三十章二十一節

人的一生常常在等待一個適當時機，做出一個正確的決定，每個人都想走一條自己的路…

四年前的某個深夜，我在中科院服務近十五年時，在決定報考博士班的剎那，其實心情是相當猶疑的！考量的原因有許多；時間上只能以半工半讀的方式攻讀，而孩子三、四歲年紀正需費心照顧，教會的服事重，且自己年近四十歲，是否還有衝勁承受修課、作研究的壓力？而學位對我的未來又有何助益？未來會走教職這條路嗎？…一念間決定的並不只是眼前四年光陰，更隱含著對未來的生涯規劃。我站在人生關鍵的十字路口，思索著該往左或往右？腦海裡反覆想著各種可能的組合，屋外漆黑的夜色逐漸被黎明的曙光染白…

四年修業時光轉眼即過，即使在研究、考試最不順心的時候也不曾後悔過，一路行來，所有的甘苦只能自己體會，而我始終堅持著那晚的抉擇。如今仍清楚記得作下決定剎那的心情，在我人生的轉折點上，勇敢堅定地，決心走出一條自己的路。

關鍵的時刻感謝有許多關鍵的人幫助了我。特別要感謝我的指導教授—郭仁財博士，他給了我學習及成長的空間，由他的身上我體會到學術研究努力不懈的態度，每當遇到瓶頸時，他的指導總為我開啟一條出路，使我能順利完成論文。謝謝諸位口試委員對論文內容的指正及建議。也要感謝實驗室夥伴們，一起研究討論，並給予我許多協助，這些回憶都深植腦海。感謝中科院五所高溫材料組長官及同仁對我的鼓勵與包容。感謝石門浸信會弟兄姊妹的代禱。

感謝自小為我操勞的雙親，在高齡九十及八十三歲的晚年仍要為我求學之路掛心，他倆的支持成為我最大的動力來源。感謝兄姊們的愛護，尤其是我的大姊，為我擔起照顧雙親的重責。最感謝的是我的妻子—林美，她全程陪我走過博士求學的路程，不論是研究受挫的苦悶抱怨，或是論文被接受的興奮喜悅，都和她一起承擔分享。當然還有我的寶貝兒子—小羽、小杰，謝謝你們給我無盡的愛。

要感謝的人太多，願將一切感謝歸給上帝，在我分不清或左或右時，祂總帶領我平安度過。

金國生 於交大
民國九十四年七月

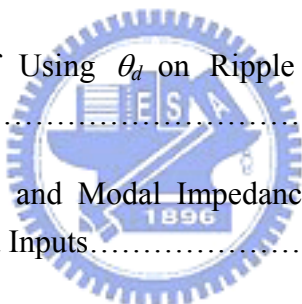
Contents

Abstract (Chinese)	I
Abstract (English)	II
Acknowledgements	III
Contents	IV
List of Tables	VI
List of Figures	VII
Chapter 1 Introduction	1
1-1 New Formulas for Synthesizing Microstrip Bandpass Filters with Relatively Wide Bandwidths.....	1
1-2 Insertion Loss Function Synthesis of Maximally Flat Parallel-Coupled Line Bandpass Filters.....	2
1-3 Direct Synthesis of Parallel-Coupled Line Bandpass Filters with Chebyshev Responses.....	3
Chapter 2 New Formulas for Synthesizing Microstrip Bandpass Filters with Relatively Wide Bandwidths	5
2-1 Design Formulas with Improved Accuracy.....	6
2-2 Filter Fabrication and Measurements.....	9
Chapter 3 Insertion Loss Function Synthesis of Maximally Flat Parallel-Coupled Line Bandpass Filters	15
3-1 The Maximally Flat Insertion Loss Function.....	16
3-1-1 First-Order Filters.....	19
3-1-2 Third-Order Filters.....	19
3-1-3 Fifth-Order Filters.....	21
3-1-4 Insertion Loss Function of a Filter of Order $N \leq 6$	22
3-1-5 The Q_T Condition and the 3-dB Bandwidth.....	24

3-2 Three Examples.....	26
3-2-1 Filter α	26
3-2-2 Filter χ	30
3-2-3 Filter β	35
3-3 Implementation Using Tapped Input/Output.....	37
3-3-1 Filter δ	38
3-3-2 Filter γ	42
Chapter 4 Direct Synthesis of Parallel-Coupled Line Bandpass Filters with Chebyshev Responses.....	44
4-1 The Chebyshev Insertion Loss Function.....	45
4-1-1 Second-Order Filters.....	46
4-1-2 Filters of Order $N \leq 5$	48
4-2 The Ripple Level and Bandwidth.....	51
4-2-1 Ripple Level Specified by θ_m	51
4-2-2 Ripple Level Specified by θ_d	52
4-3 Three Examples.....	57
4-3-1 Filter η ($N = 3, \Delta = 50\%, R = 0.5\text{dB}$).....	57
4-3-2 Filter ξ ($N = 4, \Delta = 40\%, R = 0.1\text{dB}$).....	64
4-3-3 Filter ψ ($N = 5, \Delta = 40\%, R = 0.1\text{dB}$).....	69
Chapter 5 Conclusion.....	72
Reference.....	74

List of Tables

Table 2.1	Even and Odd Mode Characteristic Impedances for the n^{th} Coupled Stages of an N^{th} -order Chebyshev Filter Obtained by the Improved and Classical Formulas. Ripple Level = 0.1dB and $\Delta= 50\%$	9
Table 3.1	The Maximally Flat Conditions for $N = 1 \sim 6$	23
Table 3.2	The Chosen Solutions and Modal Characteristic Impedances of Each Coupled Stage of Filters α , χ and β	27
Table 3.3	The Chosen Roots and Modal Impedances of the Two Experimental Filters with Tapped Inputs.....	41
Table 4.1	The Chebyshev Conditions for $N = 1 \sim 5$	50
Table 4.2	The Influences of Using θ_d on Ripple Level Design of Third-order Filters.....	56
Table 4.3	The Chosen Roots and Modal Impedances of The Three Experimental Filters with Tapped Inputs.....	63



List of Figures

Figure 2.10	(a) A coupled-line stage. (b) Equivalent circuit of (a).....	6
Figure 2.2	Normalized characteristic impedances Z_{oe} and Z_{oo} versus designed bandwidths with ripple level 0.1dB. (a) $N = 3$. (b) $N = 5$	10
Figure 2.3	Bandwidth decrement versus designed bandwidth from simulation responses of a third- and fifth-order Chebyshev filters with 0.1dB ripple level.....	12
Figure 2.4	Comparison of responses for third-order filters designed by the improved and classical formulas. The designed bandwidth is 50% and ripple level is 0.1dB. The substrate has $\epsilon_r = 10.2$ and thickness $d = 1.27\text{mm}$	13
Figure 2.5	(a) Comparison of responses for fifth-order filters designed by the improved and classical formulas. The designed bandwidth is 50% and ripple level is 0.1dB. The substrate has $\epsilon_r = 10.2$ and thickness $d = 1.27\text{mm}$. (b) Photograph of the fifth-order filter.....	14
Figure 3.1	An N -order parallel-coupled line filter.....	16
Figure 3.2	The i th coupled stage has line width W_i and gap G_i . Even and odd mode characteristic impedances are respectively Z_{oei} and Z_{ooi}	16
Figure 3.3	The calculated maximally flat responses of $N = 1, 3$ and 5 . Fractional bandwidth $\Delta = 50\%$, $f_o = 5.8\text{GHz}$	25
Figure 3.4	Possible roots for S_2 and T_2 with respect to T_1 for a third-order filter with $\Delta = 30\%$ and $\Delta = 50\%$	27
Figure 3.5	Root loci for Z_{oe} and Z_{oo} of the first and second stages of filter α when $Z_o = 50\ \Omega$ and $90\ \Omega$	28
Figure 3.6	(a) Theoretical and measured responses of filter α . (b) Photograph of the fabricated circuit. $f_o = 5.8\text{GHz}$, $N = 3$ and $\Delta = 30\%$. Circuit dimensions: $W_1 = 0.24\text{ mm}$, $G_1 = 0.15\text{ mm}$, $W_2 = 1.45\text{ mm}$, $G_2 = 0.13\text{ mm}$. The line width of the quarter-wave transformer is 0.8mm . Substrate: $\epsilon_r = 10.2$, thickness = 1.27 mm	29

Figure 3.7	Possible roots for the 2nd and 3rd coupled stages of the fifth-order filter with $\Delta = 40\%$	32
Figure 3.8	Root loci for Z_{oe} and Z_{oo} of the first, second and third stages of the fifth-order filter with $\Delta = 40\%$ and $Z_o = 50 \Omega$	33
Figure 3.9	Simulated and theoretical responses of the synthesized filter χ . $f_o = 5.8\text{GHz}$, $N = 5$, $\Delta = 40\%$. Circuit dimensions: $W_1 = 0.767 \text{ mm}$, $G_1 = 0.001 \text{ mm}$, $W_2 = 1.94 \text{ mm}$, $G_2 = 0.005 \text{ mm}$, $W_3 = 2.1 \text{ mm}$, $G_3 = 0.1 \text{ mm}$	34
Figure 3.10	Root loci of S_3 , T_3 , S_4 and T_4 for a sixth-order filter with $\Delta = 30\%$ for $(S_2, T_2) = (0.49, 0.28)$, $(0.96, 0.51)$ and $(1.54, 0.61)$	36
Figure 3.11	Simulation and theoretical responses of filter β . $f_o = 5.8\text{GHz}$, $N = 6$, $\Delta = 30\%$. Circuit dimensions: $W_1 = 0.24 \text{ mm}$, $G_1 = 0.06 \text{ mm}$, $W_2 = 1.27 \text{ mm}$, $G_2 = 0.02 \text{ mm}$, $W_3 = 0.92 \text{ mm}$, $G_3 = 0.47 \text{ mm}$, $W_4 = 0.55 \text{ mm}$, $G_4 = 0.78 \text{ mm}$	36
Figure 3.12	A tapped line treated as a two-port network.....	39
Figure 3.13	Comparison of $ S_{21} $ responses of tapped lines and coupled stages.....	39
Figure 3.14	(a) Theoretical, simulated and measured responses of filter δ . $f_o = 5.8\text{GHz}$, $N = 3$, $\Delta = 50\%$. (b) Photograph of the fabricated circuit. Circuit dimensions: $W_1 = 2\text{mm}$, $W_2 = 0.54\text{mm}$, $G_2 = 0.23\text{mm}$	40
Figure 3.15	(a) Theoretical, simulated and measured responses of filter γ . $f_o = 5.8\text{GHz}$, $N = 5$, $\Delta = 40\%$. (b) Photograph of the fabricated circuit. Circuit dimensions: $W_1 = 1.7\text{mm}$, $W_2 = 0.58\text{mm}$, $W_3 = 1.2\text{mm}$, $G_2 = 0.22\text{mm}$, $G_3 = 0.22\text{mm}$	43
Figure 4.1	Calculated Chebyshev responses with ripple levels specified by θ_m and θ_d . $N = 2$, $R = 3\text{dB}$, $\Delta = 50\%$, $f_o = 5.8 \text{ GHz}$	54
Figure 4.2	Calculated responses of third-order Chebyshev filters, with ripple levels specified by θ_d . (a) With ripple level $R = 0.5\text{dB}$. (b) With designed bandwidth $\Delta = 50\%$	55
Figure 4.3	Detailed $ S_{21} $ performance within passband of fourth-order filters with ripple levels specified by θ_d . $\Delta = 50\%$, $R = 0.1, 0.5$ and 1dB	56
Figure 4.4	Possible roots for T_1 , S_2 and T_2 with respect to k for a third-order filter	

	with $R = 0.5$ dB and $\Delta = 50\%$	59
Figure 4.5	Root loci for Z_{oe} and Z_{oo} of the first and second stages of third-order filter when $Z_o = 50 \Omega$	60
Figure 4.6	Comparison of $ S_{21} $ responses of tapped lines and coupled stages.....	61
Figure 4.7	(a) Theoretical, simulated and measured responses of filter η . (b) Photograph of the fabricated circuit. $f_o = 5.8$ GHz, $N = 3$, $\Delta = 50\%$, $R = 0.5$ dB. Circuit dimensions: $W_1 = 2$ mm, $W_2 = 0.286$ mm, $G_2 = 0.206$ mm. Substrate: $\epsilon_r = 10.2$, thickness = 1.27 mm.....	62
Figure 4.8	Possible roots for S_2 , T_2 , S_3 and T_3 with respect to T_1 for a fourth-order filter with $R = 0.1$ dB and $\Delta = 40\%$. (a) With $k = 2$. (b) With $k = 1$. (c) With $k = 0.5$	65
Figure 4.9	Root loci for Z_{oe} and Z_{oo} of the second and third stages of a fourth-order Chebyshev filter with $k = 2, 1$ and 0.5 when $Z_o = 50 \Omega$	67
Figure 4.10	(a) Theoretical, simulated and measured responses of filter ξ . $f_o = 5.8$ GHz, $N = 4$, $\Delta = 40\%$, $R = 0.1$ dB. (b) Photograph of the fabricated circuit. Circuit dimensions: $W_1 = 2$ mm, $W_2 = 0.49$ mm, $W_3 = 0.41$ mm, $G_2 = 0.23$ mm, $G_3 = 0.31$ mm.....	68
Figure 4.11	Possible roots for the 2nd and 3rd coupled stages of a fifth-order parallel-coupled line filter with $\Delta = 40\%$, $R = 0.1$ dB and $k = 0.5$	70
Figure 4.12	(a) Theoretical, simulated and measured responses of filter ψ . $f_o = 5.8$ GHz, $N = 5$, $\Delta = 40\%$, $R = 0.1$ dB. (b) Photograph of the fabricated circuit. Circuit dimensions: $W_1 = 1.97$ mm, $W_2 = 0.4$ mm, $W_3 = 0.16$ mm, $G_2 = 0.25$ mm, $G_3 = 0.39$ mm.....	71

Chapter 1

Introduction

1-1 New formulas for synthesizing microstrip bandpass filters with relatively wide bandwidths:

The ultra-wideband (UWB) technologies for commercial communication applications have created a need of a transmitter with bandwidths of up to or more than several GHz [1]. Microwave passive devices with such a wide bandwidth have been investigated recently [2–4]. Lumped elements are incorporated into the circuit design for a directional coupler with an octave-band [2]. The three-line structures in [3] and ground plane aperture compensation techniques in [4] are suitable for implementing filters of a wide bandwidth.

Consisting of a cascade of coupled stages, parallel-coupled line configuration is attractive for realizing microstrip bandpass filters in microwave frequencies [3-7]. It is popular since it has an easy synthesis procedure and a wide range of realizable bandwidths. In a conventional design, approximate synthesis formulas have been well documented for determining dimensions of each coupled stage [6-7]. In deriving these formulas, one of the key steps is to establish the equivalence of a coupled stage to a two-port network of two quarter-wave transmission line sections with an admittance inverter in between. The approximation has a good accuracy when the filter has a relatively small bandwidth. This is because the frequency response of a coupled stage has a zero derivative at center frequency f_o , and thus is relatively insensitive to variation of frequency. When the designed bandwidth becomes larger, however, the coupling of the coupled stage is no longer a constant, and it apparently rolls off as the

frequency moves away from f_o . Thus, a modification is required for the formulas when the microstrip filters are designed to have a wide bandwidth.

In Chapter 2, simple formulas are proposed for improving prediction of the bandwidth of parallel-coupled microstrip filters. Two experimental Chebyshev filters are measured to demonstrate the significant improvement.

1-2 Insertion loss function synthesis of maximally flat parallel-coupled line bandpass filters:

As mentioned in Section 1-1, since the admittance inverter in equivalent circuit is assumed independent of frequency, the conventional formulas are accurate only for bandpass filters (BPFs) with a relative small bandwidth (BW).

BPFs synthesized based on the conventional method will have a fractional BW Δ less than specification. The BW decrement deteriorates as filter order or designed BW is increased. As reported in [13], when filter order $N = 3$ and $\Delta = 35\%$, the synthesized circuit has only $\Delta = 30\%$. When $\Delta = 50\%$, the realized BWs are only 41% and 38% for $N = 3$ and $N = 5$, respectively. For recovering the BW decrement, new formulas for determining Z_{oe} and Z_{oo} of each coupled stage have been derived in Chapter 2 for synthesizing relatively wideband filters. In this way, the realized BWs can be greatly improved, but the BW decrement is still not completely resolved. For example, when $\Delta = 50\%$ is given, the new designs still have only 48.2% and 44% for $N = 3$ and $N = 5$, respectively.

Some methods have been proposed to design filters with accurate passband responses. In [14], insertion loss (IL) functions are derived for maximally flat filters with short-circuited quarter-wave stubs. The Q distribution method in [8] can provide accurate solutions to filters with narrow and wide BWs. Entire procedure for finding

the Q distribution includes choosing the number of sections, creating composite $ABCD$ matrix, and solving individual admittance values of the resonators. For direct-coupled microwave filters of 2 ~ 12 resonant elements having $\Delta = 10\% \sim 43\%$, the theoretical results in [9] have good agreement with computed responses. In [38], the synthesis formulas are derived based on the image parameter method and the insertion loss method, which are available for the design of wide-band and narrow-band microwave filters.

In Chapter 3, the IL function of a parallel-coupled bandpass filter is derived for synthesizing maximally flat responses. The synthesis formulas are derived directly from the composite $ABCD$ matrix of all coupled stages instead of using J -inverter equivalent circuits. Based on the derived function, simultaneous conditions for determining dimensions of all coupled stages are provided. Section 3-1 shows the derivation for filters of order $N \leq 6$. Section 3-2 presents results of three filters to demonstrate the formulation and synthesis. In realizing two additional relatively wideband filters, pattern resolution of certain stages exceeds our fabrication limits. Thus in Section 3-3 tapped lines are designed to resolve this problem. Measured responses are compared with EM simulation and theoretical predictions.

1-3 Direct synthesis of parallel-coupled line bandpass filters with Chebyshev responses:

The formulation in Chapter 3, however, is limited to maximally flat responses. Chebyshev filters can have more applications than those of the maximally flat type, due to the degree of freedom in trade-off between the ripple level in passband and rejection rate in transition band. Chapter 4 extends the method developed in Chapter 3 to synthesis of the Chebyshev filters. Section 4-1 formulates the IL function for filters of

order $N \leq 5$, and Section 4-2 investigates the performance of synthesized responses associated with given ripple level and BW. The IL functions can not give absolute equal ripples when $N \geq 4$. A viable method is provided to improve the situation. Section 4-3 presents three filters to demonstrate the formulation and synthesis. Measured responses are compared with theoretical predictions as well as the simulated obtained by an EM software package.



Chapter 2

New Formulas for Synthesizing Microstrip Bandpass Filters with Relatively Wide Bandwidths

Approximate design equations for each coupled stage in a parallel-coupled microstrip filter have been given by [6-7] and adopted popularly in realization. The classical design formulas for determining the dimensions of each coupled stage are derived based on an assumption that the admittance inverter is independent of frequency. As a result, these equations are accurate only for filters with relatively narrow bandwidths. Thus, for parallel-coupled microstrip filters designed to have a wide bandwidth, the design formulas need modifying.

New formulas are proposed for designing wideband parallel-coupled microstrip bandpass filters with improved prediction of bandwidth. When a fractional bandwidth Δ is required, a correction $\theta = (\pi/2)(1 \pm \Delta/2)$ is incorporated into the formulation for determining the dimensions of each coupled stage. Two filters with $\Delta = 50\%$ are designed and fabricated to show the improvement. The measurement shows a very good agreement with the simulation.

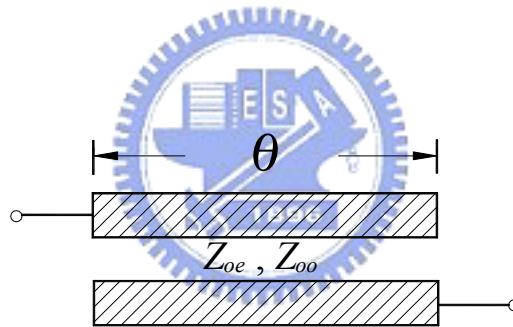
2-1 Design Formulas with Improved Accuracy

From the perspective of circuit synthesis, accurate dimensions of the coupled stage are the most important in implementing the filter. The coupled stage in Fig. 2.1(a) has an electrical length θ , and even and odd mode characteristic impedances Z_{oe} and Z_{oo} .

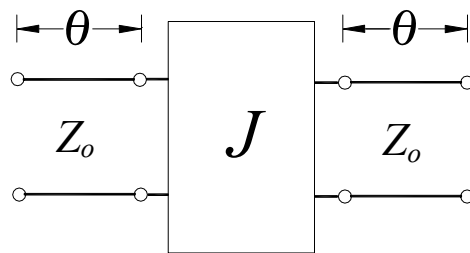
The impedance matrix elements of the coupled stage in Fig. 2.1(a) can be derived [7] as

$$Z_{11} = Z_{22} = -\frac{j}{2}(Z_{oe} + Z_{oo})\cot\theta \quad (2.1a)$$

$$Z_{12} = Z_{21} = -\frac{j}{2}(Z_{oe} - Z_{oo})\csc\theta \quad (2.1b)$$



(a)



(b)

Fig. 2.1 (a) A coupled-line stage. (b) Equivalent circuit of (a).

Here, the even- and odd-mode phase velocities for the coupled stage are assumed identical. From (2.1a) and (2.1b), the $ABCD$ matrix for the coupled-line stage can be derived as

$$\begin{bmatrix} A & B \\ C & D \end{bmatrix} = \begin{bmatrix} \frac{Z_{oe} + Z_{oo}}{Z_{oe} - Z_{oo}} \cos\theta & \frac{j}{2} \left\{ (Z_{oe} - Z_{oo}) \sin\theta - \frac{4Z_{oe}Z_{oo}}{Z_{oe} - Z_{oo}} \frac{\cos^2\theta}{\sin\theta} \right\} \\ j \frac{2}{Z_{oe} - Z_{oo}} \sin\theta & \frac{Z_{oe} + Z_{oo}}{Z_{oe} - Z_{oo}} \cos\theta \end{bmatrix} \quad (2.2)$$

The $ABCD$ matrix for the J inverter circuit in Fig. 2.1(b) can be derived as

$$\begin{aligned} \begin{bmatrix} A & B \\ C & D \end{bmatrix} &= \begin{bmatrix} \cos\theta & jZ_o \sin\theta \\ j \frac{\sin\theta}{Z_o} & \cos\theta \end{bmatrix} \begin{bmatrix} 0 & -j \\ -jJ & 0 \end{bmatrix} \begin{bmatrix} \cos\theta & jZ_o \sin\theta \\ j \frac{\sin\theta}{Z_o} & \cos\theta \end{bmatrix} \\ &= \begin{bmatrix} \left(JZ_o + \frac{1}{JZ_o} \right) \cos\theta \sin\theta & j \left(JZ_o^2 \sin^2\theta - \frac{\cos^2\theta}{J} \right) \\ j \left(\frac{1}{JZ_o^2} \sin^2\theta - J \cos^2\theta \right) & \left(JZ_o + \frac{1}{JZ_o} \right) \cos\theta \sin\theta \end{bmatrix} \end{aligned} \quad (2.3)$$

Equating the right hand sides of (2.2) and (2.3), one can express Z_{oe} and Z_{oo} in terms of the circuit parameters of the admittance inverter as follows

$$Z_{oe} = \frac{JZ_o^2 \sin\theta}{\sin^2\theta - (JZ_o \cos\theta)^2} \left[\left(JZ_o + \frac{1}{JZ_o} \right) \sin\theta + 1 \right] \quad (2.4a)$$

$$Z_{oo} = \frac{JZ_o^2 \sin\theta}{\sin^2\theta - (JZ_o \cos\theta)^2} \left[\left(JZ_o + \frac{1}{JZ_o} \right) \sin\theta - 1 \right] \quad (2.4b)$$

It is difficult to implement a coupled microstrip stage having a frequency-dependent behavior as described in (2.4). In fact, constant values for Z_{oe} and Z_{oo} have to be used to determine the dimensions of each stage from the characteristic impedance design graphs. Note that if $\theta = \pi/2$ is used, (2.4a) and (2.4b) reduce to those given in [7]. Since the approximation $\theta = \pi/2$ is accurate only in the vicinity of the center frequency, this may lead to an error in estimating the filter bandwidth. Thus, when the required fractional bandwidth is Δ ,

$$\theta = \frac{\pi}{2} \left(1 \pm \frac{\Delta}{2}\right) \quad (2.5)$$

can be used to calculate the Z_{oe} and Z_{oo} for each coupled stage. Obviously, an exact equivalence between the circuits in Fig. 2.1(a) and Fig. 2.1(b) is assured at the passband edges. This will make the prediction of filter bandwidths more accurate, which will be demonstrated later.

2-2 Filter Fabrication and Measurements

To show the significant improvement in predicting the filter bandwidth provided by (2.4) and (2.5), we first examine the changes of Z_{oe} and Z_{oo} of coupled microstrip stages due to the deviation of θ from $\pi/2$. Table 2.1 lists their values for the n^{th} coupled stage in a third-, a fifth- and a seventh-order Chebyshev filters with 0.1dB ripple level and 50% fractional bandwidth.

It is noted that for an N^{th} -order Chebyshev filter, the n^{th} coupled stage is identical to the $(N+2-n)^{\text{th}}$ one. The numbers in Table 2.1 indicate that the end stages have the largest change in Z_{oo} , which is increased by no more than 6% for all cases shown here. On the other hand, the value of Z_{oe} exhibits a significant change; for example, Z_{oe} is increased by more than 20Ω for the end stages.

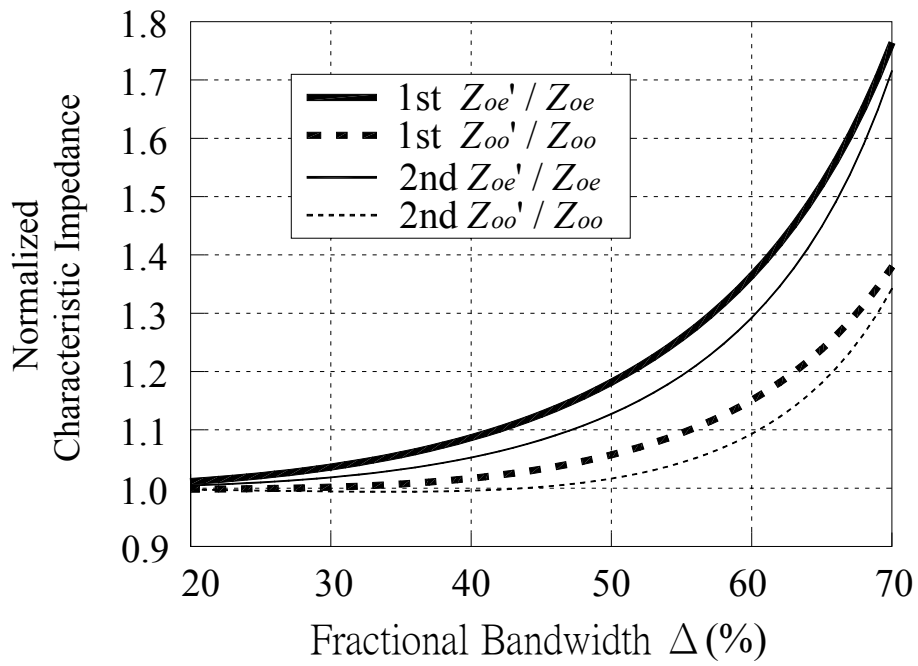


TABLE 2.1

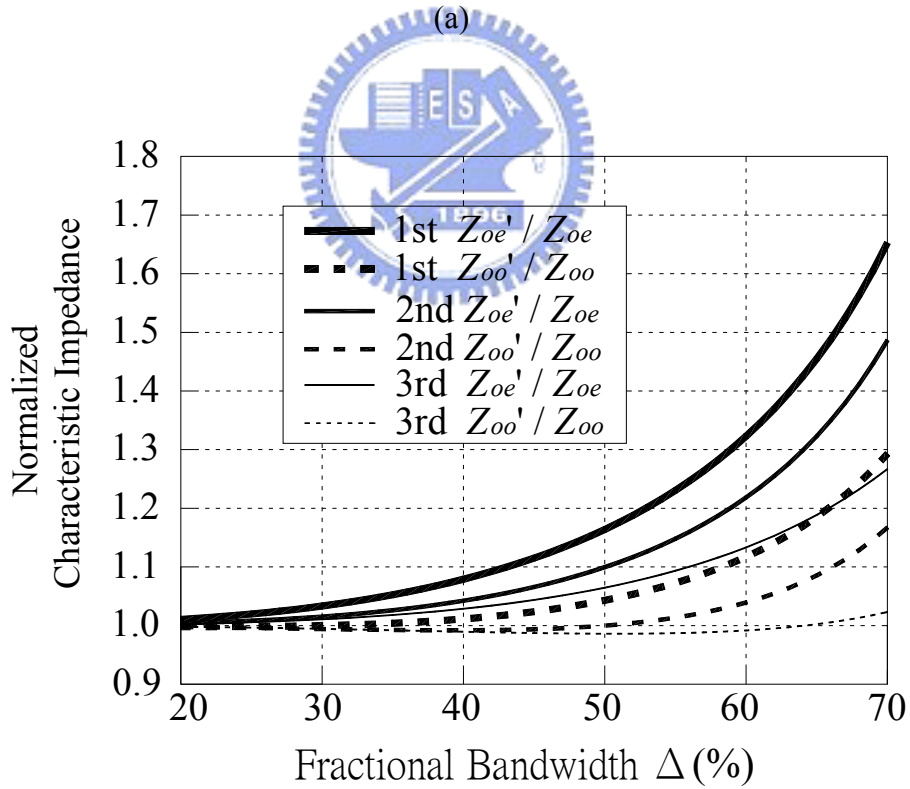
EVEN AND ODD MODE CHARACTERISTIC IMPEDANCES FOR THE n^{th} COUPLED STAGES OF AN N^{th} -ORDER CHEBYSHEV FILTER OBTAINED BY THE IMPROVED AND CLASSICAL FORMULAS.

RIPPLE LEVEL = 0.1dB AND $\Delta = 50\%$.

N	n	Improved		Classical	
		$Z_{oe}(\Omega)$	$Z_{oo}(\Omega)$	$Z_{oe}(\Omega)$	$Z_{oo}(\Omega)$
3	1	155.6	47.0	131.7	44.4
	2	126.4	40.6	112.2	40.0
5	1	146.2	44.7	125.6	42.9
	2	111.0	38.3	100.9	38.3
	3	90.8	37.0	85.3	37.5
7	1	143.8	44.2	124.0	42.5
	2	107.9	38.0	98.6	38.1
	3	88.1	37.0	83.1	37.6
	4	85.5	37.1	81.0	37.7



(a)



(b)

Figure 2.2 Normalized characteristic impedances Z_{oe} and Z_{oo} versus designed bandwidths with ripple level 0.1dB. (a) $N=3$. (b) $N=5$.

Fig. 2.2(a) and 2.2(b) show the variations of normalized characteristic impedance Z_{oe} and Z_{oo} versus designed bandwidths with Chebyshev response, ripple level 0.1dB, $N = 3$ and $N = 5$, respectively. The results are obtained by using the approximation condition (2.5). As shown in the figures, the normalized impedance Z_{oe} of each coupled stage is increased by the improved formulas, thus increased the coupling factor. The largest variation of normalized Z_{oe} is occurred at the end stage.

Next, we proceed to synthesize the parallel-coupled microstrip wideband filters. All the filters are designed on an RT/duroid 6010 substrate with $\epsilon_r = 10.2$ and thickness $d = 1.27\text{mm}$. Fig. 2.3 plots the bandwidth decrement against the designed specification. The test vehicle includes a third- and a fifth-order Chebyshev filters of ripple level 0.1dB. In simulation by the full-wave simulator IE3D [10], the responses are obtained by discretizing the circuits with twenty and forty cells per wavelength, and they are found indistinguishable.

In Fig. 2.3, the curves denoted by “classical” are of filters obtained by (2.4) with $\theta = \pi/2$, and those by “improved” are of filters synthesized by (2.4) and (2.5). When the filter order $N = 3$ and the designed bandwidth is less than 25%, the bandwidth decrement is insignificant. If Δ is increased to 35%, however, the classical formulas produce a fractional bandwidth with 5% less than the specification. The bandwidth decrement deteriorates as the filter order or the designed Δ is increased. Upon the requirement of $\Delta = 70\%$, in the classical design, the bandwidth decrements are close to 19% and 25% for $N = 3$ and $N = 5$, respectively, while in our proposed equations, the decrements are only about 5% and 12.5%.

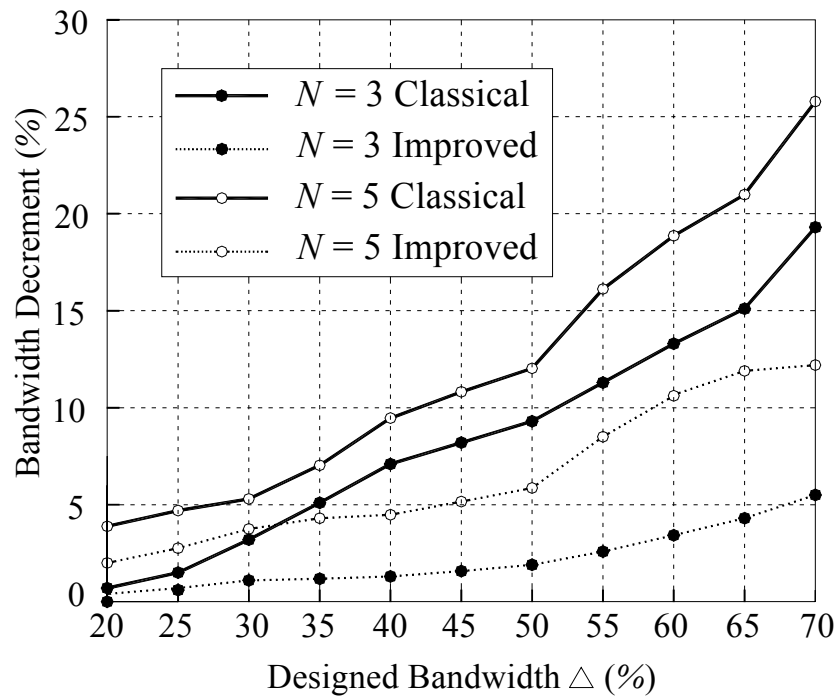
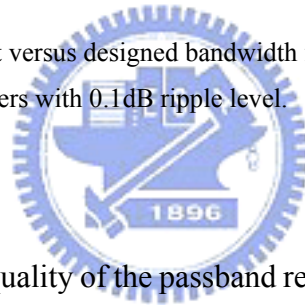


Fig. 2.3 Bandwidth decrement versus designed bandwidth from simulation responses of a third- and fifth-order Chebyshev filters with 0.1dB ripple level.



Finally, we examine the quality of the passband responses for filters designed with (2.4) and (2.5). Fig. 2.4 plots the simulation and measured responses for a third-order Chebyshev filter, and they show a very good agreement. Detailed data show that the simulated and measured results have fractional bandwidths of 48.4% and 48.2%, respectively, which are close to the designed bandwidth 50%. The measured results of a filter designed by classical formulas are also plotted for comparison. Its fractional bandwidth is only 41%.

Fig. 2.5(a) plots the results for a fifth-order filter. Again, the simulation and measured responses have a good agreement, and fractional bandwidths of 44.4% and 44%, respectively. For the filter based on the classical design, the measured response shows $\Delta = 38\%$.

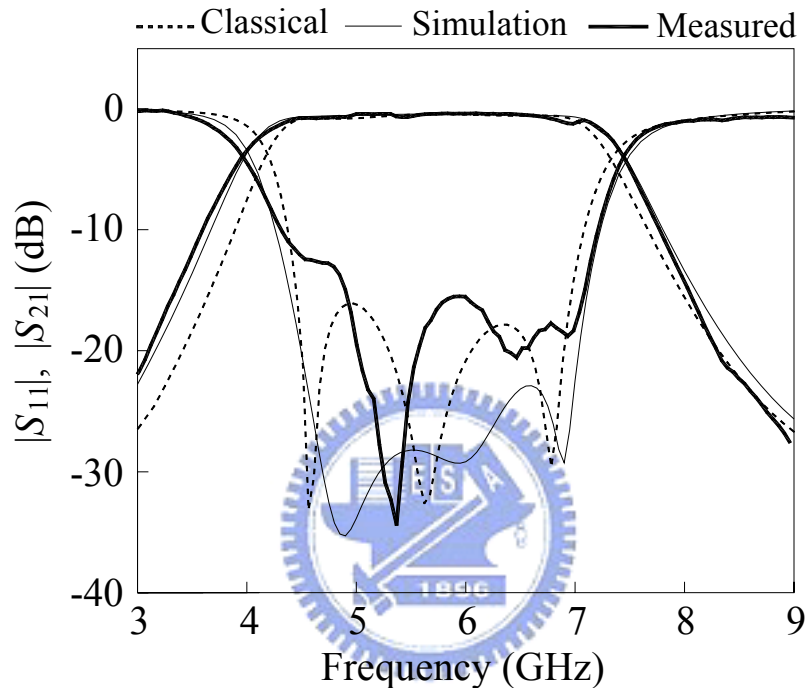
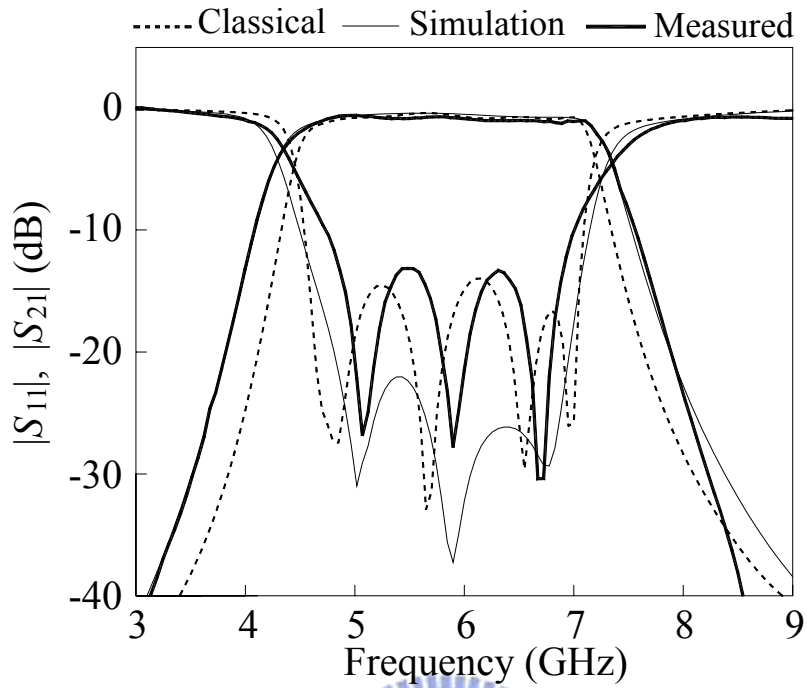
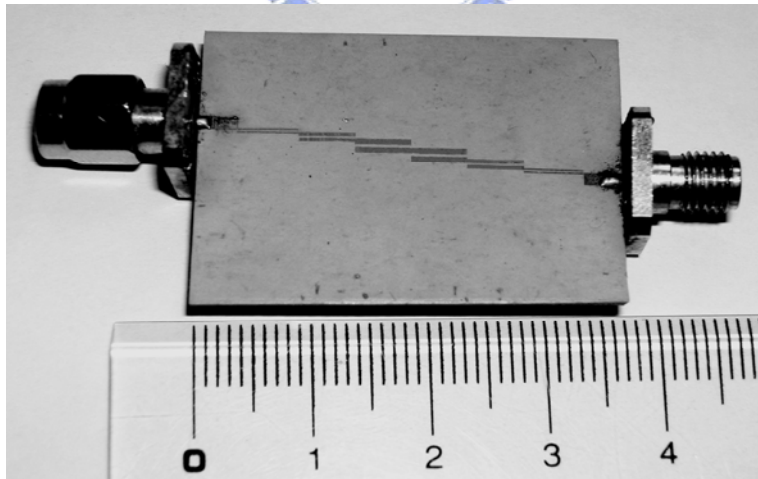


Fig. 2.4 Comparison of responses for third-order filters designed by the improved and classical formulas. The designed bandwidth is 50% and ripple level is 0.1dB. The substrate has $\epsilon_r = 10.2$ and thickness $d = 1.27\text{mm}$.



(a)



(b)

Fig. 2.5 (a) Comparison of responses for fifth-order filters designed by the improved and classical formulas. The designed bandwidth is 50% and ripple level is 0.1dB. The substrate has $\epsilon_r = 10.2$ and thickness $d = 1.27\text{mm}$. (b) Photograph of the fifth-order filter.

Chapter 3

Insertion Loss Function Synthesis of Maximally Flat Parallel-Coupled Line Bandpass Filters

Insertion loss (IL) functions are derived for synthesis of microstrip parallel-coupled line bandpass filters with maximally flat responses. The derivation is performed by successively multiplying the $ABCD$ matrices of all coupled stages instead of using J -inverter equivalent circuits. Simultaneous equations for determining line width and line spacing of the coupled stages are established by total Q (Q_T) of the filter specification and comparing the IL function with the canonical form. The results are provided for filters of order $N \leq 6$. Two filters with fractional bandwidths $\Delta = 30\%$ and a filter with $\Delta = 40\%$ are synthesized and demonstrated by simulation using an EM full-wave software package, while measurements are further performed for one of them. The results show very accurate bandwidths. The under-determined conditions leave several degrees of freedom in choosing the circuit dimensions. By properly utilizing these degrees of freedom, the problem resulted from the tight coupled-line dimensions can be resolved by gathering all difficulties to the end stages and employing tapped input/output to replace the end stages. Two filters with $\Delta = 40\%$ and 50% are fabricated to proof the feasibility. The measured results show very good agreement with the theoretical responses.

3-1 The Maximally Flat Insertion Loss Function

For the N -order parallel-coupled microstrip filter in Fig. 3.1, let the generator and load impedances be identical and normalized to unity. Since a maximally flat response is assumed, the circuit layout is symmetric about its center and, when it is characterized by a composite $ABCD$ matrix, $A = D$ holds. It can be shown that the IL function can be written as [6]

$$\frac{P_o}{P_L} = 1 + \left[\frac{j(B-C)}{2} \right]^2 = 1 + (\Omega^N)^2 \quad (3.1)$$

where $j = \sqrt{-1}$, N is order, P_o is power available from source, and P_L is power delivered to load.

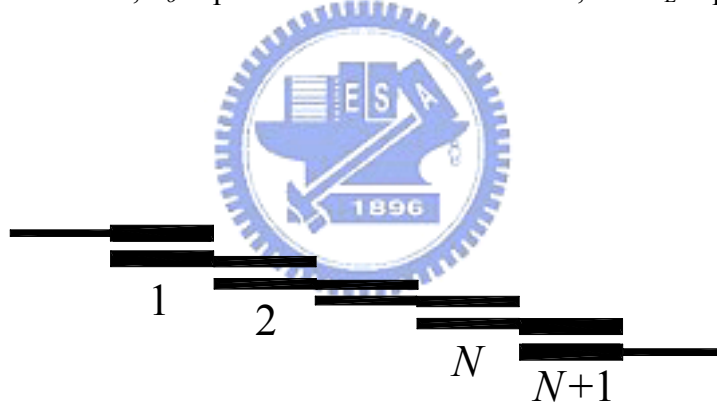


Fig. 3.1 An N -order parallel-coupled line filter.

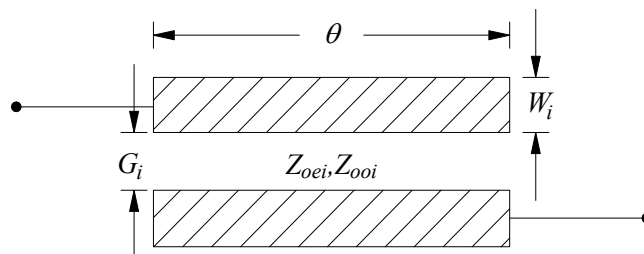


Fig. 3.2 The i th coupled stage has line width W_i and gap G_i . Even and odd mode characteristic impedances are respectively Z_{oei} and Z_{ooi} .

Of an N th-order filter, the impedance matrix elements of the i th coupled stage in Fig. 3.2 can be derived [7] as

$$Z_{11i} = Z_{22i} = -\frac{j}{2}(Z_{oei} + Z_{ooi})\cot\theta \quad (3.2a)$$

$$Z_{12i} = Z_{21i} = -\frac{j}{2}(Z_{oei} - Z_{ooi})\csc\theta \quad (3.2b)$$

where θ is its electrical length and Z_{oei} and Z_{ooi} are the characteristic impedances of the even- and odd-modes, respectively. Here, the even- and odd-mode phase velocities for all coupled stages are assumed identical. From (3.2a) and (3.2b), the $ABCD$ matrix can be obtained as

$$\begin{bmatrix} A_i & B_i \\ C_i & D_i \end{bmatrix} = \frac{\sin\theta}{T_i} \begin{bmatrix} qS_i & \frac{j}{2}[T_i^2 + q^2(T_i^2 - S_i^2)] \\ 2j & qS_i \end{bmatrix} \quad (3.3a)$$

$$q = \cot\theta \quad (3.3b)$$

$$S_i = \frac{Z_{oei} + Z_{ooi}}{Z_o} \quad (3.3c)$$

$$T_i = \frac{Z_{oei} - Z_{ooi}}{Z_o} \quad (3.3d)$$

The composite $ABCD$ matrix of an N -order filter can be obtained by successively multiplying the $N+1$ $ABCD$ matrices as follows:

$$\begin{bmatrix} A & B \\ C & D \end{bmatrix}_N = \begin{bmatrix} A_1 & B_1 \\ C_1 & D_1 \end{bmatrix} \begin{bmatrix} A_2 & B_2 \\ C_2 & D_2 \end{bmatrix} \cdots \begin{bmatrix} A_{N+1} & B_{N+1} \\ C_{N+1} & D_{N+1} \end{bmatrix} \quad (3.4)$$

As N becomes large, the result of (3.4) can be very tedious and complicated. If the matrix entries are expressed in terms of q , however, the results become much simpler. Substituting (3.3a) for all stages into (3.4) yields

$$\begin{bmatrix} A & B \\ C & D \end{bmatrix}_N = \frac{\sin^{N+1} \theta}{T_1 T_2 \dots T_{N+1}} \times \begin{bmatrix} f_a(q) & f_b(q) \\ f_c(q) & f_d(q) \end{bmatrix} \quad (3.5a)$$

Where

$$\begin{bmatrix} f_a(q) & f_b(q) \\ f_c(q) & f_d(q) \end{bmatrix} = \begin{bmatrix} a_0 + q^2 a_2 + \dots + q^{N+1} a_{N+1} & \frac{j}{2} [q b_1 + q^3 b_3 + \dots + q^{N+2} b_{N+2}] \\ 2j [q c_1 + q^3 c_3 + \dots + q^N c_N] & d_0 + q^2 d_2 + \dots + q^{N+1} d_{N+1} \end{bmatrix} \quad (3.5b)$$

when N is odd, and



$$\begin{bmatrix} f_a(q) & f_b(q) \\ f_c(q) & f_d(q) \end{bmatrix} = \begin{bmatrix} q a_1 + q^3 a_3 + \dots + q^{N+1} a_{N+1} & \frac{j}{2} [b_0 + q^2 b_2 + \dots + q^{N+2} b_{N+2}] \\ 2j [c_0 + q^2 c_2 + \dots + q^N c_N] & q d_1 + q^3 d_3 + \dots + q^{N+1} d_{N+1} \end{bmatrix} \quad (3.5c)$$

when N is even. The coefficients of each polynomial are functions of S_i and T_i . The object of (3.5) is to find conditions for determining Z_{oei} and Z_{ooi} , and hence geometries of the coupled stages.

3-1-1 First-order Filters:

When $N = 1$, the composite $ABCD$ matrix is a product of two identical $ABCD$ matrices. It can be derived that

$$\begin{aligned} & \frac{j(B-C)}{2} \\ &= \frac{1}{T_1^2} \left[\sin \theta \cos \theta (2S_1 - \frac{1}{2} S_1^3) + \frac{\cos \theta}{\sin \theta} \frac{S_1}{2} (S_1^2 - T_1^2) \right] \end{aligned} \quad (3.6)$$

Comparing (3.6) with the canonical form (3.1), we have

$$2S_1 - \frac{1}{2} S_1^3 = 0 \quad \text{or} \quad S_1 = 2 \quad (3.7)$$

Substituting (3.7) into (3.6) yields the IL function

$$\frac{P_o}{P_L} = 1 + \left[\frac{\cos \theta}{\sin \theta} \right]^2 \left[\frac{S_1(S_1^2 - T_1^2)}{2T_1^2} \right]^2 \quad (3.8)$$

The condition for solving T_1 can be obtained by imposing the given 3-dB bandwidth to (3.8). This will be addressed later.

3-1-2 Third-order Filters:

For a third-order filter, $S_1 = S_4$, $S_2 = S_3$, $T_1 = T_4$, and $T_2 = T_3$. The composite $ABCD$ matrix can be obtained by multiplying the $ABCD$ matrices of the leading two stages, and post-multiplying the resulted matrix by itself with indices 1 and 2 being

interchanged. The result can be written as

$$\begin{aligned} \frac{j(B-C)}{2} &= \frac{-1}{2T_1^2 T_2^2} [\sin \theta \cos \theta (h_1) \\ &+ \sin \theta \cos^3 \theta (h_2 - h_1 - h_3) + \frac{\cos^3 \theta}{\sin \theta} (h_3)] \end{aligned} \quad (3.9a)$$

Where

$$h_1 = 4T_2^2 (S_1 + S_2) - T_1^2 (S_1 T_2^2 + S_2 T_1^2) \quad (3.9b)$$

$$\begin{aligned} h_2 &= -2T_1^2 (S_1 T_2^2 + S_2 T_1^2) + (S_1 + S_2) \times \\ &(T_2^2 S_1^2 + 2T_1^2 S_1 S_2 + 4T_2^2 - 4S_2^2 - 4S_1 S_2) \end{aligned} \quad (3.9c)$$

$$\begin{aligned} h_3 &= (T_1^2 - S_1^2) S_1 S_2^2 - S_2 (T_1^2 - S_1^2)^2 \\ &+ (T_2^2 - S_2^2) [S_1^2 S_2 - S_1 T_1^2 + S_1^3] \end{aligned} \quad (3.9d)$$

Matching (3.9a) with the canonical form (3.1), we reserve only the $\cos^3 \theta / \sin \theta$ term, i.e., enforce $h_1 = 0$ and $h_2 = h_3$, to eliminate the dependence of the IL function on $\sin \theta \cos \theta$ and $\sin \theta \cos^3 \theta$. It leads to the following two conditions:

$$S_1 = 2 \quad (3.10a)$$

$$4T_2^2 (S_1 + S_2) = T_1^2 (S_1 T_2^2 + S_2 T_1^2) \quad (3.10b)$$

Inserting (3.10b) and (3.9d) into (3.9a) yields

$$\frac{P_o}{P_L} = 1 + \left[\frac{\cos^3 \theta}{\sin \theta} \right]^2 \left[\frac{2S_2 (S_1 + S_2) [(S_1 + S_2) - T_1^2]}{T_1^2 T_2^2} \right]^2 \quad (3.11)$$

The variable S_1 is purposely kept in (3.11) since it is useful in expressing the IL function in a general form. Note that there are four unknowns to be determined by only three equations, i.e., (3.10a), (3.10b), and (3.11) from given BW. Thus we have one degree of freedom in choosing the circuit dimensions.

3-1-3 Fifth-order Filters:

When $N = 5$, from the circuit symmetry, $S_1 = S_6$, $S_2 = S_5$, $S_3 = S_4$, $T_1 = T_6$, $T_2 = T_5$ and $T_3 = T_4$. It can be derived that

$$\frac{j(B-C)}{2} = \frac{-1}{2T_1^2 T_2^2 T_3^2} [\sin\theta \cos\theta(g_1) + \sin\theta \cos^3\theta(g_2 - 2g_1) + \sin\theta \cos^5\theta(g_1 - g_2 + g_3 - g_4) + \frac{\cos^5\theta}{\sin\theta}(g_4)] \quad (3.12a)$$

where

$$g_1 = T_2^2 T_3^2 [S_1 T_1^2 - 4(S_1 + S_2)] + T_1^4 T_3^2 (S_2 + S_3) - 4S_3 T_2^4 \quad (3.12b)$$

$$g_2 = (T_3^2 - S_3^2)[(S_2 + S_3)T_1^4 - 4S_2 T_2^2] + T_3^2 (T_1^2 - S_1^2)[S_1 T_2^2 + 2(S_2 + S_3)T_1^2] - 4(T_2^2 - S_2^2)(S_2 T_3^2 + 2S_3 T_2^2) - (T_1^2 - 4)[S_1 S_2 T_3^2 (S_2 + 2S_3) + S_1 S_3 T_2^2 (2S_2 + S_3)] + S_1 (T_1^2 - 4)[(T_2^2 - S_2^2)T_3^2 + (T_3^2 - S_3^2)T_2^2] + 4T_3^2 [S_2^2 S_3 + S_1^2 (S_2 + S_3)] - S_2 S_3 T_1^4 (S_2 + S_3) + T_2^2 (4S_2 S_3^2 - S_1^2 S_2 T_3^2 - S_1^2 S_3 T_2^2) \quad (3.12c)$$

$$g_3 = (T_1^2 - S_1^2)(T_3^2 - S_3^2)[2T_1^2 (S_2 + S_3) + S_1 T_2^2] - (T_1^2 - S_1^2)[S_1 S_2 T_3^2 (S_2 + 2S_3) + S_1 S_3 T_2^2 (2S_2 + S_3) + 2S_2 S_3 T_1^2 (S_2 + S_3)] + (T_2^2 - S_2^2)(4S_2 S_3^2 - S_1^2 S_2 T_3^2 - 2S_1^2 S_3 T_2^2) + (T_3^2 - S_3^2)[S_2 (4S_2 S_3 - S_1^2 T_2^2) + 4S_1^2 (S_2 + S_3)] - S_1 S_2 (T_3^2 - S_3^2)(T_1^2 - 4)(S_2 + 2S_3) - S_1 S_3 (T_2^2 - S_2^2)(T_1^2 - 4)(2S_2 + S_3) - 4S_2 (T_2^2 - S_2^2)(T_3^2 - S_3^2) + S_1 T_3^2 (T_1^2 - S_1^2)(T_2^2 - S_2^2) + S_1 (T_1^2 - 4)(T_2^2 - S_2^2)(T_3^2 - S_3^2) - 4S_3 (T_2^2 - S_2^2)^2 + T_3^2 (T_1^2 - S_1^2)^2 (S_2 + S_3) + S_1 S_2 S_3^2 (T_1^2 - 4) + S_1^2 S_2 S_3 [S_3 T_2^2 + S_2 T_3^2 - 4(S_2 + S_3)] \quad (3.12d)$$

$$g_4 = S_1 S_2^2 S_3^2 (T_1^2 - S_1^2) + S_1^2 S_2 S_3^2 (T_2^2 - S_2^2) + S_1^2 S_2^2 S_3 (T_3^2 - S_3^2) - S_1 S_2 (S_2 + 2S_3)(T_1^2 - S_1^2)(T_3^2 - S_3^2) - S_1 S_3 (2S_2 + S_3)(T_1^2 - S_1^2)(T_2^2 - S_2^2) - S_1^2 S_2 (T_2^2 - S_2^2)(T_3^2 - S_3^2) + (S_2 + S_3)(T_1^2 - S_1^2)^2 (T_3^2 - S_3^2 - S_2 S_3) - S_1^2 S_3 (T_2^2 - S_2^2)^2 + S_1 (T_1^2 - S_1^2)(T_2^2 - S_2^2)(T_3^2 - S_3^2) \quad (3.12e)$$

Matching (3.12a) with the canonical form (3.1), we reserve only the $\cos^5\theta/\sin\theta$ term, i.e., enforce $g_1 = 0$, $g_2 = 2g_1$ and $g_1 - g_2 + g_3 - g_4 = 0$ to eliminate the dependence of the IL function on $\sin\theta\cos\theta$, $\sin\theta\cos^3\theta$ and $\sin\theta\cos^5\theta$. It leads to the following three conditions:

$$S_1 = 2 \quad (3.13a)$$

$$4T_2^2[T_3^2(S_1 + S_2) + S_3T_2^2] = T_1^2T_3^2[S_1T_2^2 + T_1^2(S_2 + S_3)] \quad (3.13b)$$

$$8T_2^2S_3(S_1 + S_2) + 4T_3^2(S_1 + S_2)^2 = T_1^2[T_1^2S_3(S_2 + S_3) + 2T_2^2S_1S_3 + 2T_3^2S_1(S_1 + S_2)] \quad (3.13c)$$

Inserting (3.13b) and (3.13c) into (3.12a) yields the IL function as

$$\frac{P_o}{P_L} = 1 + \left[\frac{\cos^5\theta}{\sin\theta} \right]^2 \left[\frac{2S_3(S_1 + S_2)(S_2 + S_3)^2[(S_1 + S_2) - T_1^2]}{T_1^2T_2^2T_3^2} \right]^2 \quad (3.14)$$

Note that in (3.14) there are six unknowns, i.e., S_1 , S_2 , S_3 , T_1 , T_2 , and T_3 , to be determined. When the circuit bandwidth is given, there are only four conditions including (3.13a) ~ (3.13c). It means that we have two degrees of freedom in choosing the circuit dimensions.

3-1-4 Insertion Loss Function of a Filter of Order $N \leq 6$:

For an N th-order filter, the IL function can be derived in a similar fashion. The simultaneous equations for solving S_i and T_i are obtained by saving $\cos^N\theta/\sin\theta$ term and enforcing coefficients for all other terms to zero. It is found that a general expression exists for the IL functions of order $N \leq 6$:

$$\frac{P_o}{P_L} = 1 + \left[\frac{\cos^N \theta}{\sin \theta} \right]^2 [K_N]^2 \quad (3.15a)$$

$$K_N = \left| \frac{\prod_{i=1}^N (S_i + S_{i+1}) - \prod_{i=1}^{N-1} (S_i + S_{i+1}) T_1^2}{T_1 T_2 \dots T_{N+1}} \right| \quad (3.15b)$$

It is interesting to note that in the θ -dependent term of (3.15a), the numerator is $\cos^{2N}\theta$ and denominator is $\sin^2\theta$. The former reflects the fact that the leading $2N - 1$ derivatives of (3.15a) with respect to θ are zero at f_o , and the latter implies a transmission zero existing at $2f_o$ where $\theta = \pi$. The zero relies on the assumption that all coupled-line stages in the filter have only one phase velocity.

The simultaneous conditions for determining S_i and T_i are listed in Table 3.1. It is found that $S_1 = 2$ for each N . Note that total number of unknowns for an N -order filter is $N+1$ for odd N and $N+2$ for even N . As shown in Table 3.1, only $[N/2] + 2$ conditions are obtained, including the condition specified by the bandwidth. Here, $[N/2]$ is an integer by truncating $N/2$. It can be seen that number of equations is less than that of unknowns when $N \geq 2$. For example, when $N = 6$, eight variables have to be found for four of seven coupled stages. Three free dimensions exist since these variables are specified by only five equations. This under-determined feature is very helpful for circuit realization since both line width and gap size of coupled microstrips have resolution limits in fabrication. This will be discussed in Section 3-3.

TABLE 3.1
THE MAXIMALLY FLAT CONDITIONS FOR $N = 1 \sim 6$.

N	Maximally Flat Conditions	Degree of Freedom
1	$S_1 = 2$	0
2	$S_1 = 2$ $2T_2 = T_1^2$	1
3	$S_1 = 2$ $4T_2^2(S_1 + S_2) = T_1^2(S_1T_2^2 + S_2T_1^2)$	1
4	$S_1 = 2$ $2T_2^2 = T_1^2T_3$ $[2T_3(S_1 + S_2) + T_1^2(S_2 + S_3)]^2 = 2T_1^2[T_1^2(S_2 + S_3)^2 + T_2^2S_1(S_2 + S_3) + T_3^2S_1(S_1 + S_2)]$	2
5	$S_1 = 2$ $4T_2^2[T_3^2(S_1 + S_2) + S_3T_2^2] = T_1^2T_3^2[S_1T_2^2 + T_1^2(S_2 + S_3)]$ $8T_2^2S_3(S_1 + S_2) + 4T_3^2(S_1 + S_2)^2 = T_1^2[T_1^2S_3(S_2 + S_3) + 2T_2^2S_1S_3 + 2T_3^2S_1(S_1 + S_2)]$	2
6	$S_1 = 2$ $2T_2^2T_4 = T_1^2T_3^2$ $4[T_2^2(S_3 + S_4) + T_3^2(S_1 + S_2)]^2 = 2T_1^2T_3^2[T_1^2(S_2 + S_3)(S_3 + S_4) + T_2^2S_1(S_3 + S_4) + T_3^2S_1(S_1 + S_2)]$ $+ T_4^2(S_2 + S_3)[T_1^4(S_2 + S_3) + 2T_1^2T_2^2S_1 - 8T_2^2(S_1 + S_2)]$ $4(S_1 + S_2)(S_2 + S_3)[2T_2^2(S_3 + S_4) + 2T_3^2(S_1 + S_2) + T_4^2(S_1 + S_2)]$ $= T_1^2[T_1^2(S_2 + S_3)(S_3 + S_4)^2 + 2T_2^2S_1(S_3 + S_4)^2 + 4T_3^2S_1(S_1 + S_2)(S_3 + S_4) + 2T_4^2S_1(S_1 + S_2)(S_2 + S_3)]$	3

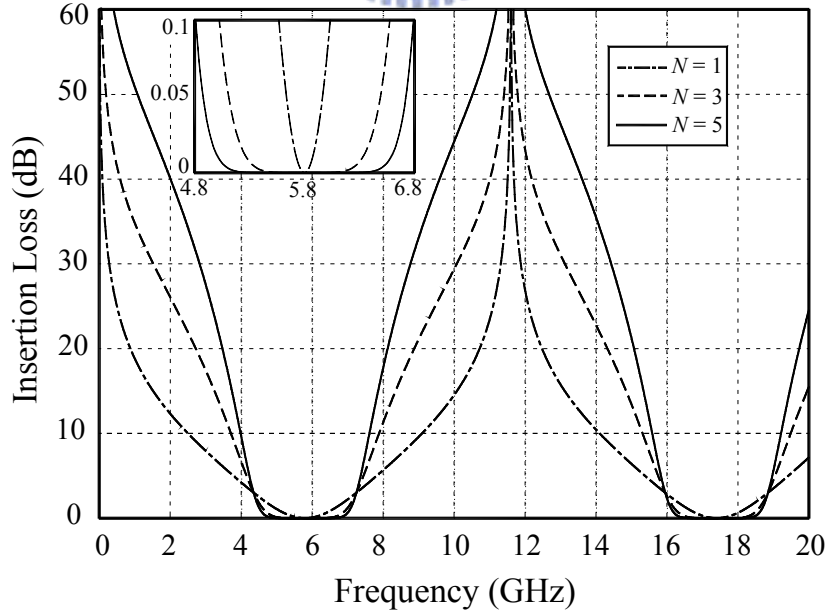


Fig. 3.3 The calculated maximally flat responses of $N=1, 3$ and 5 . Fractional bandwidth $\Delta=50\%$, $f_o=5.8$ GHz.

3-1-5 The Q_T Condition and the 3-dB Bandwidth:

For a maximally flat filter, the total Q (Q_T) and the 3-dB bandwidth is related by

$$Q_T = \frac{\omega_0}{\omega_2 - \omega_1} \quad (3.16)$$

where ω_0 is the design frequency, and ω_1 and ω_2 are the 3-dB cutoff frequencies specified by

$$\left. \frac{P_L}{P_o} \right|_{\omega_1, \omega_2} = \frac{1}{2} \quad (3.17)$$

Thus, the electrical length θ can be written in terms of Q_T as

$$\left. \theta \right|_{\omega_1, \omega_2} = \frac{\pi}{2} \left(1 \pm \frac{1}{2Q_T} \right) \quad (3.18)$$

and K_N in (3.15a) can be derived as

$$K_N \Big|_{\omega_1, \omega_2} = \left| \frac{\sin \theta}{\cos^N \theta} \right|_{\omega_1, \omega_2} \quad (3.19)$$

This is called the Q_T condition herein. For demonstration, based on (3.15a) and (3.19), Fig. 3.3 plots the calculated maximally flat responses for $N = 1, 3$ and 5 with $\Delta = 50\%$ and $f_o = 5.8\text{GHz}$. The inserted frame shows the detailed passband performance.

The synthesis method can be applied to Chebyshev filters as well. For example, when $N = 3$, the expressions of h_1, h_2 , and h_3 in (3.9a) are then specified by constants associated with the ripple level. Detailed results will be reported later in Chapter 4.

3-2 Three Examples

A third-order filter α and a sixth-order filter β are synthesized with $\Delta = 30\%$, and the fifth-order filter χ is synthesized with $\Delta = 40\%$ for validating the formulation. The center frequency is $f_o = 5.8\text{GHz}$. Simulated results by the IE3D [10] are presented for three circuits, while measurements are further performed for filter α .

3-2-1 Filter α :

When $N = 3$, the Q_T condition (3.19) gives

$$2S_2(2 + S_2)[(2 + S_2) - T_1^2] = \left| \frac{\sin \theta}{\cos^3 \theta} \right| T_1^2 T_2^2 \quad (3.20)$$

where (3.10a) is used and, from (3.18), $\theta = 1.3352$ radian. Inserting (3.10b) into (3.20) yields

$$8(2 + S_2)^3 - 12(2 + S_2)^2 T_1^2 + 4(2 + S_2) T_1^4 - \left| \frac{\sin \theta}{\cos^3 \theta} \right| T_1^6 = 0 \quad (3.21)$$

There is one degree of freedom in finding the solution. Fig. 3.4 plots the solutions of S_2 and T_2 for T_1 ranging from 0.9 to 1.3. Referring to (3.3c) and (3.3d), we have $Z_{oei} = (S_i + T_i) \times Z_o / 2$ and $Z_{ooi} = (S_i - T_i) \times Z_o / 2$. Obviously, not all roots shown in Fig. 3.4 are realizable using the standard microstrip technology. Realizable Z_{oei} and Z_{ooi} depend on structural parameters, and obviously Z_o is the dominant factor. Suppose that the filters are designed on a substrate with $\epsilon_r = 10.2$ and thickness $d = 1.27\text{mm}$. According to resolution of our fabrication facilities, G/d and W/d must be no less than 0.1. When $Z_o = 50\Omega$ and 90Ω , Z_{oe} and Z_{oo} for the first and second stages are plotted together with the design graph in Fig. 3.5. As T_1 is increased, values of Z_{oe1} , Z_{oe2} , and Z_{oo2} increase while that of Z_{oo1} decreases. If $Z_o = 50\Omega$ is used, the gap size G/d for stage 1 will be no larger than 0.1. If both stages are required to have $G/d \geq 0.1$, for $Z_o = 90\Omega$, value of T_1 must be between 1.03 and 1.06. Therefore, the solution is chosen as $S_1 = 2$, $T_1 = 1.043$, $S_2 = 0.895$ and $T_2 = 0.336$. The corresponding modal characteristic impedances are listed in Table 3.2.

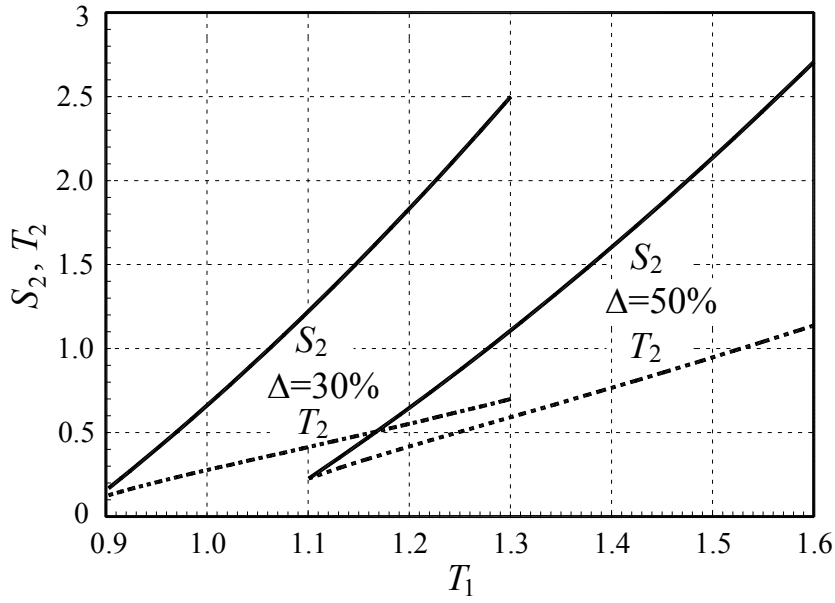


Fig. 3.4 Possible roots for S_2 and T_2 with respect to T_1 for a third-order filter with $\Delta = 30\%$ and $\Delta = 50\%$.



TABLE 3.2

THE CHOSEN SOLUTIONS AND MODAL CHARACTERISTIC IMPEDANCES OF EACH COUPLED STAGE OF FILTERS α , χ AND β

Filters	1st stage	2nd stage	3rd stage	4th stage
α $N = 3$ $\Delta = 30\%$ $Z_o = 90\Omega$	$S_1 = 2$ $T_1 = 1.043$ $Z_{oe1} = 136.93\Omega$ $Z_{oo1} = 43.07\Omega$	$S_2 = 0.895$ $T_2 = 0.336$ $Z_{oe2} = 55.40\Omega$ $Z_{oo2} = 25.16\Omega$	Same as the 2nd stage	Same as the 1st stage
χ $N = 5$ $\Delta = 40\%$ $Z_o = 50\Omega$	$S_1 = 2$ $T_1 = 1.454$ $Z_{oe1} = 86.35\Omega$ $Z_{oo1} = 13.65\Omega$	$S_2 = 1.32$ $T_2 = 0.72$ $Z_{oe2} = 51\Omega$ $Z_{oo2} = 15\Omega$	$S_3 = 1.321$ $T_3 = 0.447$ $Z_{oe3} = 44.2\Omega$ $Z_{oo3} = 21.85\Omega$	Same as the 3rd stage
β $N = 6$ $\Delta = 30\%$ $Z_o = 90\Omega$	$S_1 = 2$ $T_1 = 1.23$ $Z_{oe1} = 145.35\Omega$ $Z_{oo1} = 34.65\Omega$	$S_2 = 0.96$ $T_2 = 0.51$ $Z_{oe2} = 66.15\Omega$ $Z_{oo2} = 20.25\Omega$	$S_3 = 1.25$ $T_3 = 0.4$ $Z_{oe3} = 74.25\Omega$ $Z_{oo3} = 38.25\Omega$	$S_4 = 1.65$ $T_4 = 0.465$ $Z_{oe4} = 95.18\Omega$ $Z_{oo4} = 53.33\Omega$

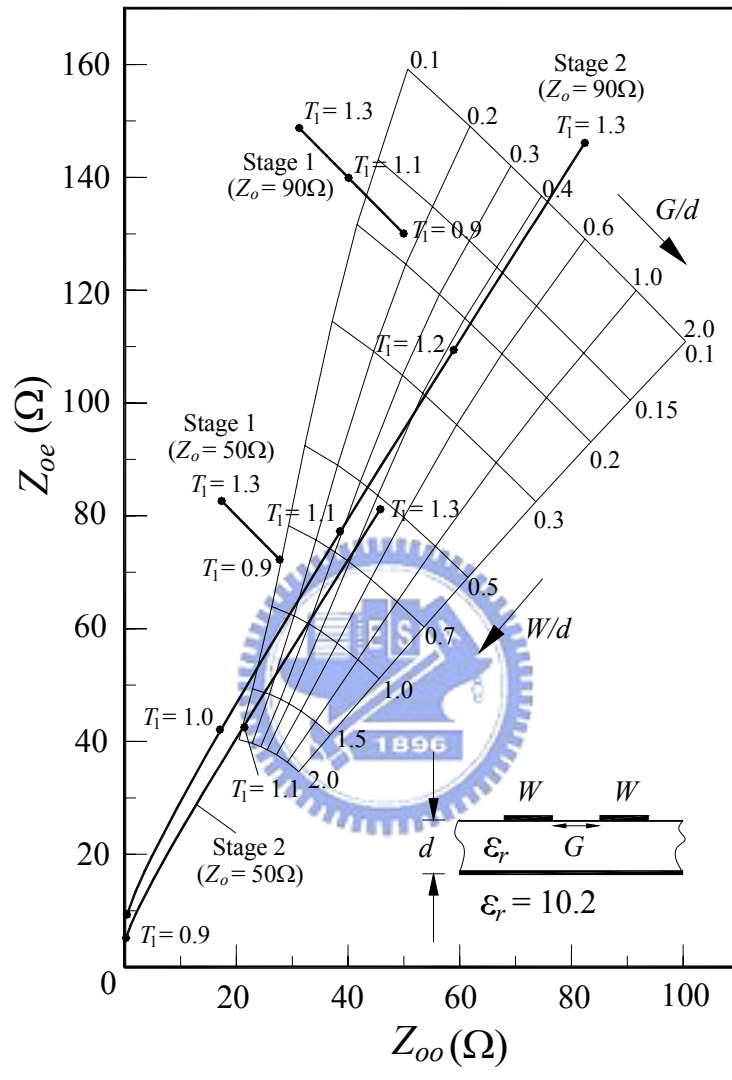
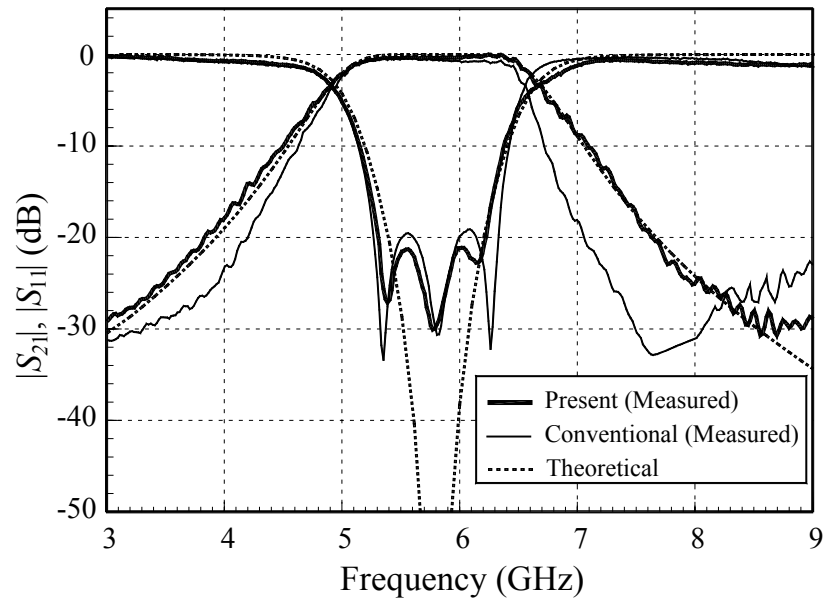
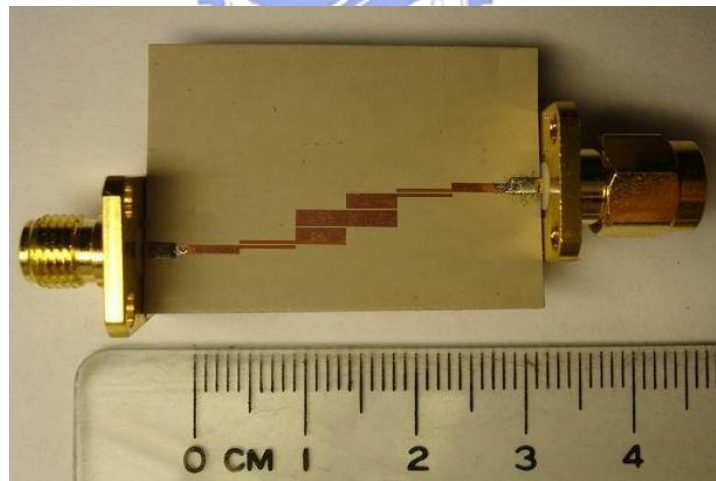


Fig. 3.5 Root loci for Z_{oe} and Z_{oo} of the first and second stages of filter α when $Z_o = 50 \Omega$ and 90Ω .



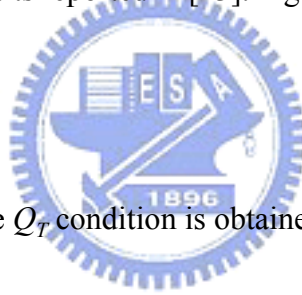
(a)



(b)

Fig. 3.6 (a) Theoretical and measured responses of filter α . (b) Photograph of the fabricated circuit. $f_o = 5.8\text{GHz}$, $N = 3$ and $\Delta = 30\%$. Circuit dimensions: $W_1 = 0.24\text{ mm}$, $G_1 = 0.15\text{ mm}$, $W_2 = 1.45\text{ mm}$, $G_2 = 0.13\text{ mm}$. The line width of the quarter-wave transformer is 0.8mm . Substrate: $\epsilon_r = 10.2$, thickness = 1.27 mm .

Fig. 3.6(a) shows the theoretical and measured results of filter α . Quarter-wave transformers are used to match $Z_o = 90 \Omega$ to 50Ω at the input and output ports. In Fig. 3.6(a), the curve denoted by “theoretical” is obtained by (3.11), and those by “present” and “conventional” are measured responses of filters synthesized by the present method and the conventional method [7], respectively. The “present” response matches with the “theoretical” maximally flat response very well. The excess poles of $|S_{11}|$ could result from the unequal even- and odd-mode phase velocities of the microstrip coupled stages. Detailed data show that the measured “present” filter has $\Delta = 30.2\%$, very close to the design. The filter based on the conventional method [6-7] has $\Delta = 26\%$, mainly due to the use of frequency independent J -inverters for the coupled-line stages. This is consistent with the results reported in [13]. Fig. 3.6(b) is photograph of filter α .



3-2-2 Filter χ :

For a fifth-order filter, the Q_T condition is obtained as

$$2S_3(S_1 + S_2)(S_2 + S_3)^2[(S_1 + S_2) - T_1^2] = \left| \frac{\sin \theta}{\cos^5 \theta} \right| T_1^2 T_2^2 T_3^2 \quad (3.22)$$

Using (3.22) and the maximally conditions (3.13a) ~ (3.13c), the maximally flat responses are well specified. From (3.18), $\theta = 1.2566$ radian. There are two degrees of freedom for choosing the solutions. Fig. 3.7 plots the filtered solutions of S_2 , T_2 , S_3 and T_3 for T_1 ranging from 1.4 to 1.75. When $Z_o = 50 \Omega$, Z_{oe} and Z_{oo} for the first, second and third stages are plotted together with the design graph in Fig. 3.8. It is found the gap size G/d for stage 1 is always less than 0.1 even the degrees of freedom in choosing the

solution are fully utilized. However, we choose a solution for the 5-order filter for validating the circuit synthesis. The characteristic impedances for each coupled stages are listed in Table 3.2 and detailed dimensions are in the figure caption of Fig. 3.9. Since some gap sizes, $G_1 = 0.001$ mm and $G_2 = 0.005$ mm, are far beyond the best resolution of our fabrication facilities, only simulation responses are provided. Fig. 3.9 shows the theoretical and simulated results of this filter. If the conventional method is used, upon the requirement of $\Delta = 40\%$, the bandwidth decrement could close to 10% [13]. While in our proposed method, the bandwidth is 40.5% which very close to the specification.



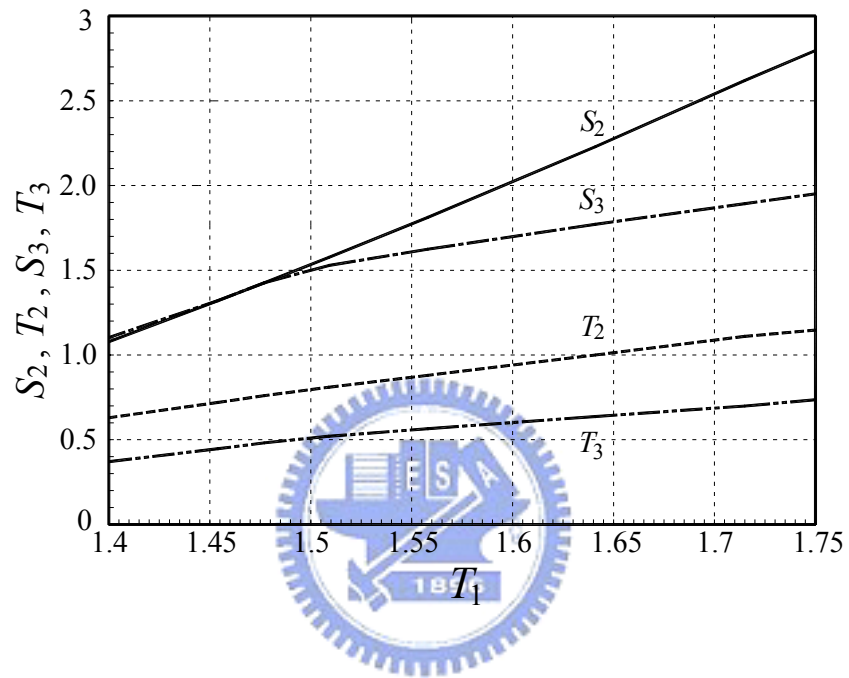


Fig. 3.7 Possible roots for the 2nd and 3rd coupled stages of the fifth-order filter with $\Delta = 40\%$.

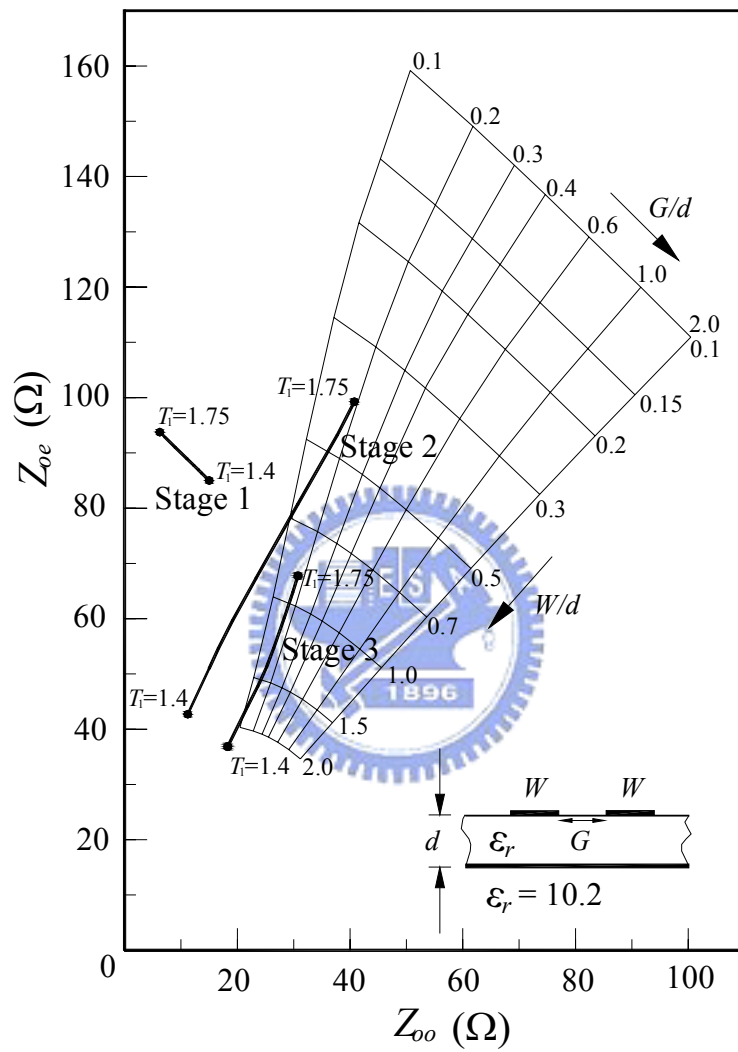


Fig. 3.8 Root loci for Z_{oe} and Z_{oo} of the first, second and third stages of the fifth-order filter with $\Delta = 40\%$ and $Z_o = 50 \Omega$.

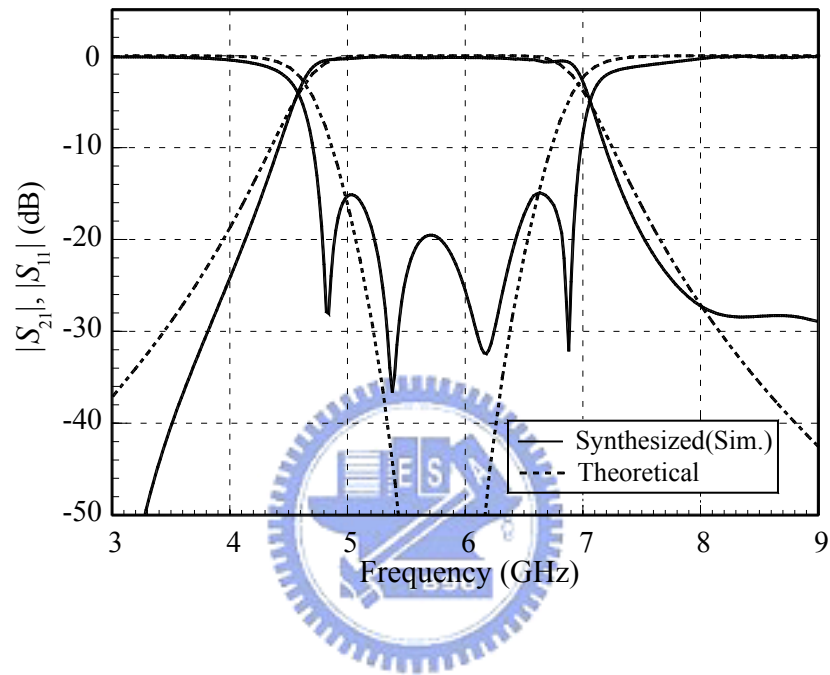


Fig. 3.9 Simulated and theoretical responses of the synthesized filter $\chi.f_o = 5.8\text{GHz}$, $N = 5$, $\Delta = 40\%$.
 Circuit dimensions: $W_1 = 0.767\text{ mm}$, $G_1 = 0.001\text{ mm}$, $W_2 = 1.94\text{ mm}$, $G_2 = 0.005\text{ mm}$, $W_3 = 2.1\text{ mm}$, $G_3 = 0.1\text{ mm}$.

3-2-3 Filter β :

For a sixth-order filter, the Q_T condition is

$$(2 + S_2)(S_2 + S_3)^2(S_3 + S_4)^2[(2 + S_2) - T_1^2] = \left| \frac{\sin \theta}{\cos^6 \theta} \right| T_1^2 T_2^2 T_3^2 T_4 \quad (3.23)$$

There are three degrees of freedom for choosing the solutions. We take T_1 , S_2 and T_2 as sweep variables in solving the simultaneous equations. If solutions with tough structural parameters are removed, the rest S_2 ranges from 0.49 to 1.54 and T_2 from 0.28 to 0.61, for $1.08 \leq T_1 \leq 1.7$. Three sets of solutions with $(S_2, T_2) = (0.49, 0.28)$, $(0.96, 0.51)$ and $(1.54, 0.61)$ are plotted in Fig. 3.10. Based on the design graph in Fig. 3.5 and $Z_o = 90\Omega$, we choose a solution for filter β for validating the circuit synthesis. As shown in Fig. 3.11, the simulation results match very well with the theoretical prediction. The simulated response has a BW of 30.3%, i.e., only 0.3% away from the specification. The characteristic impedances for each coupled stage are listed in Table 3.2 and detailed dimensions are in the figure caption. Since some gap sizes, $G_1 = 0.06\text{mm}$ and $G_2 = 0.02\text{mm}$, are far beyond the best resolution of our fabrication facilities, only simulation responses are provided.

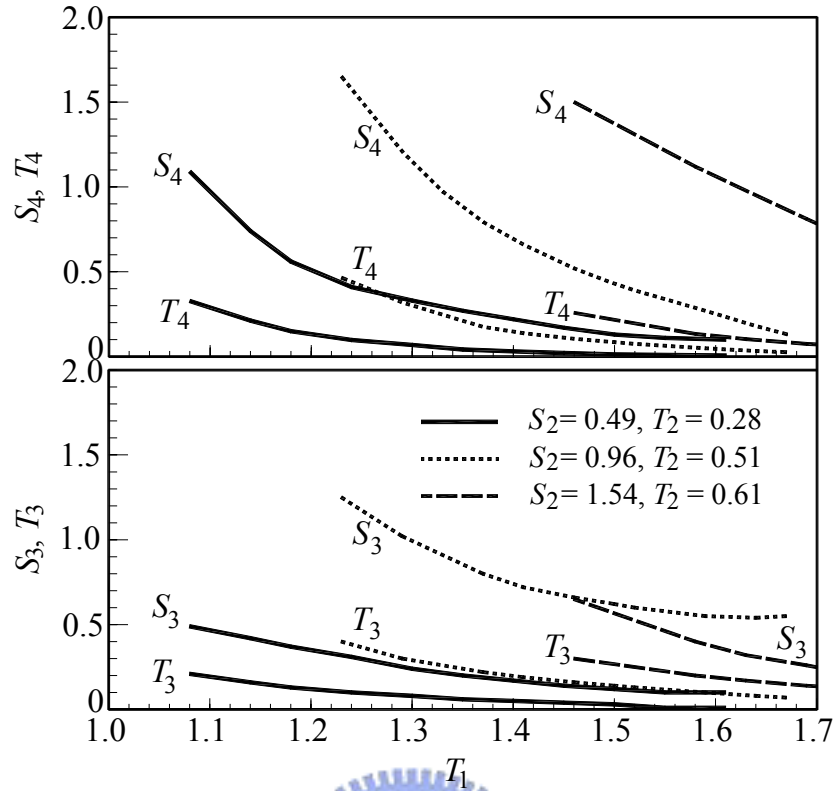


Fig. 3.10 Root loci of S_3 , T_3 , S_4 and T_4 for a sixth-order filter with $\Delta = 30\%$ for $(S_2, T_2) = (0.49, 0.28)$, $(0.96, 0.51)$ and $(1.54, 0.61)$.

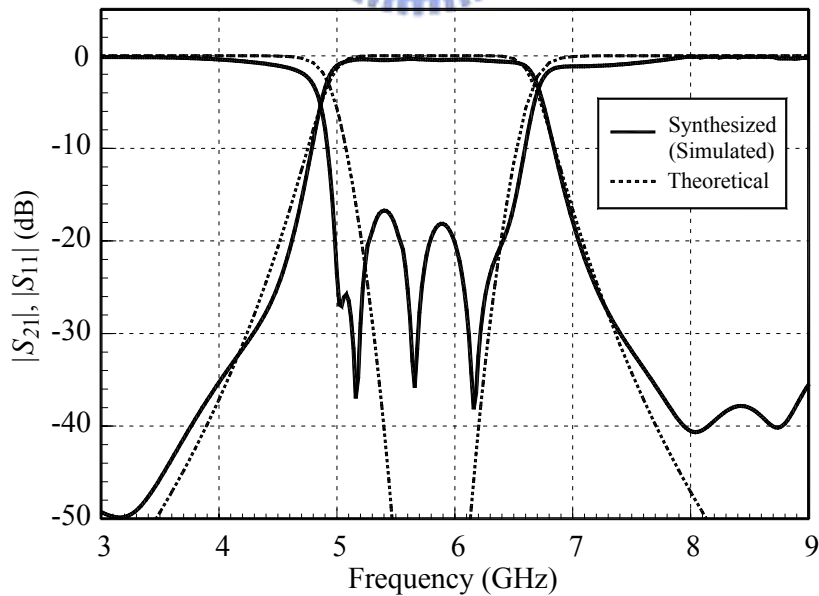
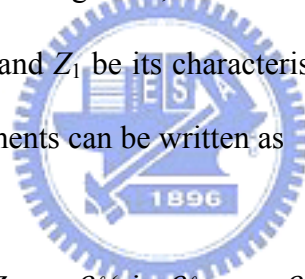


Fig. 3.11 Simulation and theoretical responses of filter β . $f_o = 5.8\text{GHz}$, $N = 6$, $\Delta = 30\%$. Circuit dimensions: $W_1 = 0.24\text{ mm}$, $G_1 = 0.06\text{ mm}$, $W_2 = 1.27\text{ mm}$, $G_2 = 0.02\text{ mm}$, $W_3 = 0.92\text{ mm}$, $G_3 = 0.47\text{ mm}$, $W_4 = 0.55\text{ mm}$, $G_4 = 0.78\text{ mm}$.

3-3 Implementation Using Tapped Input/Output

In many cases, such as Fig. 3.11, line widths or gaps are too small to fabricate, even the degrees of freedom in choosing the solution are fully utilized. This situation becomes more severe when order or BW is increased. Fortunately, the tapped input/output [15-16] can be used to resolve this problem. Theoretically, the tapping structure can realize a very wide range of the coupling coefficients. Thus, criterion for choosing the solution becomes to release dimensions of middle stages and locate the difficulties to the end stages as much as possible.

Since the derivation of the IL function (3.15) is based on a cascade of coupled stages, we have to establish the equivalence between a tapped resonator and a coupled stage. For the tapped structure in Fig. 3.12, let ℓ be the distance between the tap point and one end of the resonator and Z_1 be its characteristic impedance. It can be shown that its impedance matrix elements can be written as



$$Z_{11} = -jZ_1 \cos \beta\ell (\sin \beta\ell + \cos \beta\ell \cot \beta L) \quad (3.24a)$$

$$Z_{12} = Z_{21} = -j \frac{Z_1 \cos \beta\ell}{\sin \beta L} \quad (3.24b)$$

$$Z_{22} = -jZ_1 \cot \beta L \quad (3.24c)$$

At the same time, the Z matrix elements of a coupled-line stage are (3.2a) and (3.2b). The equivalence of these two two-ports can be established by letting $\theta = \beta L = \pi/2$, $\ell = 0$ and $Z_1 = (Z_{oe} - Z_{oo})/2$. The equivalence is, however, valid only for a finite frequency band. Fig. 3.13 investigates the performance of the equivalence. Two coupled stages with $(Z_{oe}, Z_{oo}) = (92.88\Omega, 7.12\Omega)$ and $(89.68\Omega, 10.32\Omega)$ are studied. The sum of Z_{oe}

and Z_{oo} is 100Ω since $S_1 = 2$ and $Z_o = 50\Omega$ is expected. In Fig. 3.13, both cases have a maximal $|S_{21}|$ deviation less than 0.08 dB and 0.34 dB within a BW of 50% and 100%, respectively. These two tapped line structures will be employed to the following two experimental filters.

3-3-1 Filter δ :

This filter is designed to have $N = 3$ and $\Delta = 50\%$. Based on (3.18), $\theta = 1.1781$ radian, the S_2 and T_2 solutions for T_1 varying from 1.1 to 1.6 are shown in Fig. 3.4. For realization, the chosen roots and modal impedances are listed in Table 3.3 with $Z_o = 50\Omega$. A tapped resonator with $Z_1 = 39.68\Omega$ is used to replace the end stages with $Z_{oe1} = 89.68\Omega$ and $Z_{oo1} = 10.32\Omega$. Fig. 3.14(a) plots the theoretical, simulated and measured responses. They have very good agreement within the passband. Detailed data show that the BWs of the simulated and measured results have only 0.5% and -0.5%, respectively, away from the theory. The measured midband insertion loss is about 0.35dB. Photograph of the fabricated filter is in Fig. 3.14(b). Note that the line gap 0.23mm is much easier to realize than the 0.13mm-gap of filter α . Thus, as compared with filter α , there are at least two advantages incorporating the tapped input/output into the design. One is that it greatly releases the tough circuit dimensions even though the BW is increased from 30% to 50%, and the other is that the impedance transformer can be saved since $Z_o = 50\Omega$.

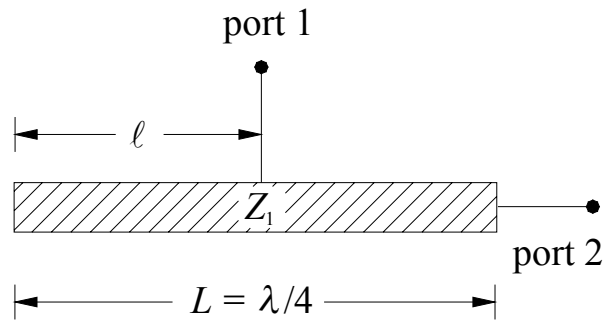


Fig.3.12 A tapped line treated as a two-port network.

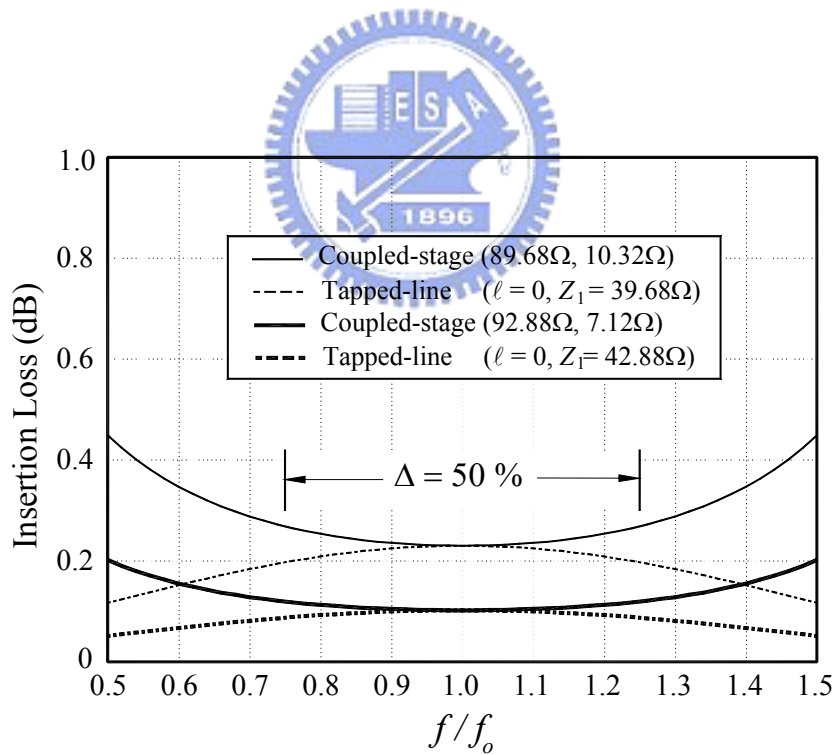
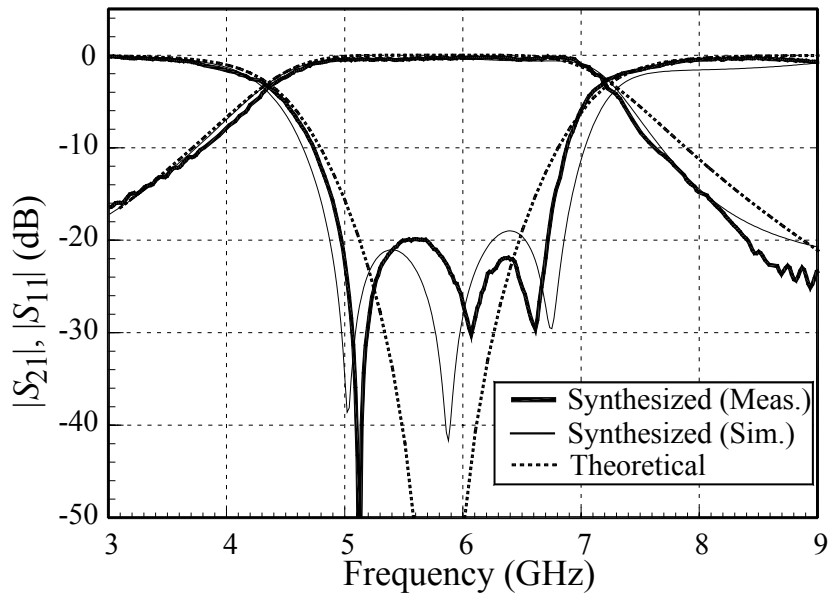


Fig. 3.13 Comparison of $|S_{21}|$ responses of tapped lines and coupled stages.



(a)



(b)

Fig. 3.14 (a) Theoretical, simulated and measured responses of filter $\delta.f_o = 5.8\text{GHz}$, $N = 3$, $\Delta = 50\%$. (b) Photograph of the fabricated circuit. Circuit dimensions: $W_1 = 2\text{mm}$, $W_2 = 0.54\text{mm}$, $G_2 = 0.23\text{mm}$.

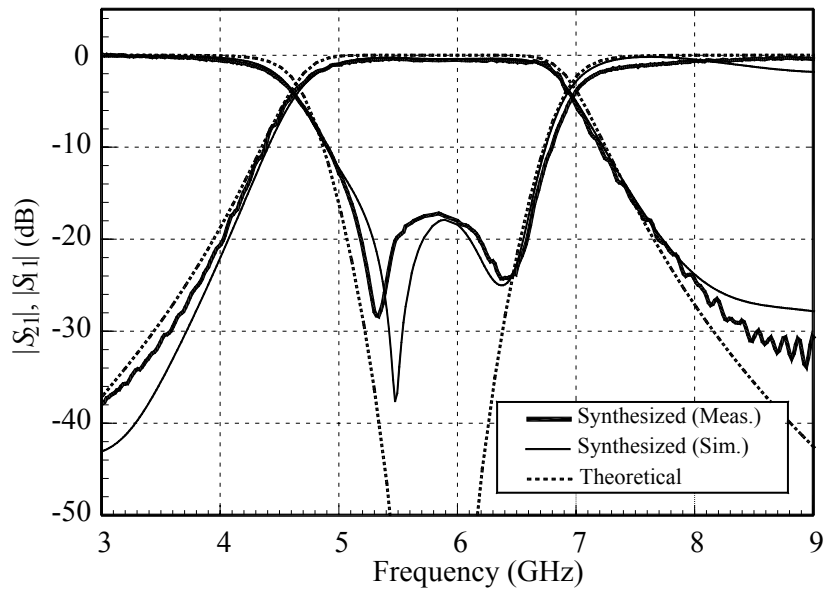
TABLE 3.3
THE CHOSEN ROOTS AND MODAL IMPEDANCES OF THE TWO EXPERIMENTAL FILTERS
WITH TAPPED INPUTS

Filters	1 st stage	2 nd stage	3 rd stage
δ $N = 3$ $\Delta = 50\%$ $Z_o = 50\Omega$	$S_1 = 2$ $T_1 = 1.587$ $\ell = 0$ $Z_1 = 39.68\Omega$	$S_2 = 2.629$ $T_2 = 1.112$ $Z_{oe2} = 93.53\Omega$ $Z_{oo2} = 37.93\Omega$	Same as the 2nd stage
γ $N = 5$ $\Delta = 40\%$ $Z_o = 50\Omega$	$S_1 = 2$ $T_1 = 1.715$ $\ell = 0$ $Z_1 = 42.88\Omega$	$S_2 = 2.619$ $T_2 = 1.11$ $Z_{oe2} = 93.23\Omega$ $Z_{oo2} = 37.73\Omega$	$S_3 = 1.893$ $T_3 = 0.699$ $Z_{oe3} = 64.80\Omega$ $Z_{oo3} = 29.85\Omega$

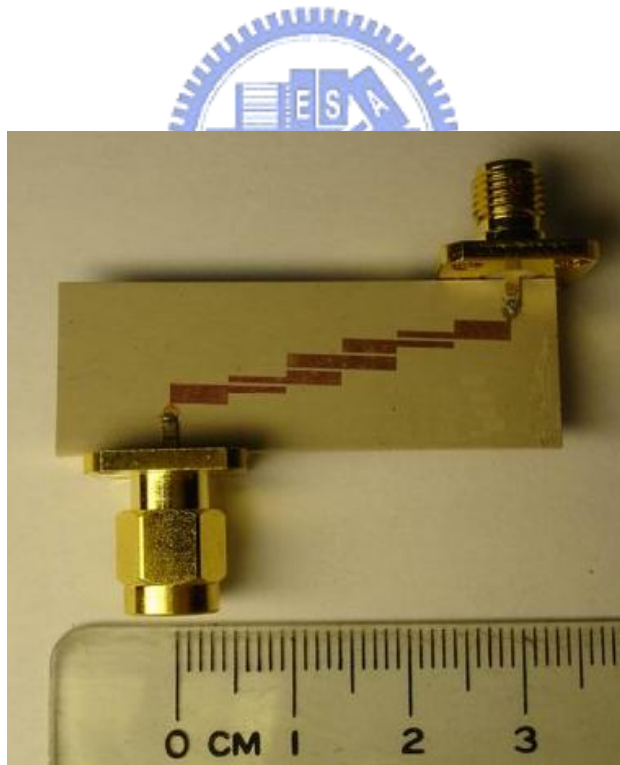
3-3-2 Filter γ :

The second experiment is a fifth-order filter with $\Delta = 40\%$. Fig. 3.7 plots the filtered roots with $\theta = 1.2566$ radian. The end stages, with $Z_{oe1} = 92.88\Omega$ and $Z_{oo1} = 7.12\Omega$, are replaced with a tapped resonator with $Z_1 = 42.88\Omega$. Fig. 3.15(a) plots the theoretical, simulation and measured results. All of them show good agreement. The measured midband insertion loss is 0.5dB. The BW of the measured response has about 1% less than the theoretical calculation by (3.15). The required minimal gap of this filter is 0.22mm. If a coupled stage is used instead, the required line gap will be less than 0.01mm. Fig. 3.15(b) is the photograph of the experiment circuit.





(a)



(b)

Fig. 3.15 (a) Theoretical, simulated and measured responses of filter $\gamma.f_o = 5.8\text{GHz}$, $N = 5$, $\Delta = 40\%$. (b) Photograph of the fabricated circuit. Circuit dimensions: $W_1 = 1.7\text{mm}$, $W_2 = 0.58\text{mm}$, $W_3 = 1.2\text{mm}$, $G_2 = 0.22\text{mm}$, $G_3 = 0.22\text{mm}$.

Chapter 4

Direct Synthesis of Parallel-Coupled Line Bandpass Filters with Chebyshev Responses

Parallel-coupled line filters with Chebyshev responses are synthesized based on derived insertion loss (IL) function method. The synthesis provides improvement in prediction of circuit bandwidth. The IL function is obtained by converting the product of the $ABCD$ matrices of all coupled stages. Simultaneous equations for Chebyshev filters of order $N \leq 5$ are derived for calculating geometric parameters of the coupled stages associated with specific in-band ripple levels. The results are provided for filters of order $N \leq 5$. Emphasis is also placed on the trade-off between fractional bandwidth Δ and in-band ripple level. When $N \geq 4$, the passband response is specified by a maximal ripple level. A filter with fractional bandwidths $\Delta = 50\%$ and two filters with $\Delta = 40\%$ are fabricated and demonstrated by simulation using an EM full-wave software package. Tapped line inputs are employed to these circuits since line widths or gaps for certain stages are beyond the common fabrication resolution. The measured results show very good agreement with the theoretical responses.

4-1 The Chebyshev Insertion Loss Function

Let both the generator and load impedances of the synthesized circuit be normalized with respect to system impedance Z_o and identical to unity. The $ABCD$ matrix of the i th coupled stage in Fig. 3.2 can be written as

$$\begin{bmatrix} A_i & B_i \\ C_i & D_i \end{bmatrix} = \frac{\sin \theta}{T_i} \begin{bmatrix} qS_i & \frac{j}{2}[T_i^2 + q^2(T_i^2 - S_i^2)] \\ 2j & qS_i \end{bmatrix} \quad (4.1)$$

where $j = \sqrt{-1}$, θ is its electrical length, $q = \cot \theta$, $S_i = (Z_{oei} + Z_{ooi})/Z_o$, $T_i = (Z_{oei} - Z_{ooi})/Z_o$, and Z_{oei} and Z_{ooi} are the characteristic impedances for the even- and odd-modes, respectively, of the coupled lines. The line width W_i and gap G_i are target variables to be solved by the synthesis. Here, the even- and odd-mode phase velocities for all coupled stages are assumed identical.

The composite $ABCD$ matrix of an N th-order filter can be obtained by successively performing N multiplications of the $N + 1$ $ABCD$ matrices. As reported in Chapter 3, each matrix entry is a finite power series of q with coefficients that are functions of S_i and T_i . Since the circuit is symmetric, it can be shown that the IL function can be written as

$$\frac{P_o}{P_L} = 1 - \frac{(B - C)^2}{4} \quad (4.2)$$

where P_o is power available from source and P_L is power delivered to load. The general insertion loss function for a Chebyshev filter can be expressed as

$$\frac{P_o}{P_L} = 1 + \varepsilon^2 [\mathbf{T}_N(x)]^2 \quad (4.3)$$

where $1 + \varepsilon^2$ is the ripple level and $\mathbf{T}_N(x)$ is the Chebyshev polynomial of order N of the first kind. The object of (4.2) is to match (4.3) and hence to establish simultaneous conditions for determining Z_{oei} and Z_{ooi} .

4-1-1 Second-order Filters:

As an example, the insertion loss function of a second-order Chebyshev filter is derived. When $N = 2$, the composite $ABCD$ matrix involves two matrix multiplications. From the circuit symmetry, $S_1 = S_3$ and $T_1 = T_3$. It can be derived that

$$\frac{j(B - C)}{2} = \frac{1}{2T_1^2 T_2 \sin \theta} \times \left[-h_1 + \cos^2 \theta (2h_1 - h_2) + \cos^4 \theta (-h_1 + h_2 - h_3) \right] \quad (4.4a)$$

where

$$h_1 = 2T_2^2 - \frac{T_1^4}{2} \quad (4.4b)$$

$$h_2 = S_1 T_1^2 (S_1 + S_2) - 2(S_1 + S_2)^2 - T_1^4 + \frac{S_1^2 T_2^2}{2} + 2T_2^2 \quad (4.4c)$$

$$h_3 = S_1 T_1^2 (S_1 + S_2) - \frac{S_1^2}{2} (S_1 + S_2)^2 - \frac{T_1^4}{2} + \frac{S_1^2 T_2^2}{2} \quad (4.4d)$$

Substituting (4.4a) into (4.2), the insertion loss function can be written as

$$\frac{P_o}{P_L} = 1 + \left[\frac{1}{2T_1^2 T_2 k \sin \theta} \right]^2 \times \left[-kh_1 + kx^2 \cos^2 \theta_m (2h_1 - h_2) + k \cos^4 \theta (-h_1 + h_2 - h_3) \right]^2 \quad (4.5a)$$

where

$$x = \frac{\cos \theta}{\cos \theta_m} \quad (4.5b)$$

$$\theta_m = \frac{\pi}{2} \left(1 \pm \frac{1}{2Q_T} \right) \quad (4.5c)$$

In (4.5c), Q_T is the total Q of the filter and θ_m is the electrical length of a coupled stage at passband edges. A variable k is purposely added in (4.5a), since it provides an extra freedom in matching coefficients in (4.5a) with (4.3) and preserves the given Chebyshev response at the same time. Note that x in (4.5b) defines the mapping $\theta = \theta_m$ to $x = 1$.

Substituting $\mathbf{T}_2(x)$ into (4.3), the insertion loss function can be written as

$$\frac{P_o}{P_L} = 1 + \varepsilon^2 [\mathbf{T}_2(x)]^2 = 1 + \varepsilon^2 (2x^2 - 1)^2 \quad (4.6)$$

Matching (4.5a) with (4.6) and enforcing $kh_1 = 1$, $k \cos^2 \theta_m (2h_1 - h_2) = 2$ and $h_2 = h_1 + h_3$.

It leads to the following three conditions:

$$S_1 = 2 \quad (4.7a)$$

$$2T_2^2 - \frac{T_1^4}{2} = \frac{1}{k} \quad (4.7b)$$

$$(S_1 + S_2)[S_1 T_1^2 - 2(S_1 + S_2)] = -\frac{2}{k \cos^2 \theta_m} \quad (4.7c)$$

Inserting (4.7a) ~ (4.7c) into (4.5a) yields

$$\frac{P_o}{P_L} = 1 + \left[\frac{1}{2T_1^2 T_2 k \sin \theta} \right]^2 [\mathbf{T}_2(x)]^2 \quad (4.8)$$

The term $[\mathbf{T}_2(x)]^2$ will provide an equal ripple response in the passband, and its coefficient $[2T_1^2 T_2 k \sin \theta]^{-1}$ not only defines the ripple level but also implies a transmission zero at $2f_o$ where $\theta = \pi$. Due to the frequency variable $1/\sin \theta$, the uniformity of the ripple levels is deteriorated when $N \geq 4$. This point will be addressed in Section 4-2. Note that in (4.7a) ~ (4.7c) there are five unknowns, i.e., k, S_1, S_2, T_1 and T_2 , to be determined. By imposing the given ripple level to (4.8), the system has four conditions. If in (4.5a) the variable k is not introduced, the system will be fully determined.

4-1-2 Filters of Order $N \leq 5$:

For an N th-order parallel-coupled line filter, the IL function can be derived in a similar fashion. Note that it needs $N+1$ 2×2 matrix products obtain the composite $ABCD$ matrix. When N is large, the expressions for the matrix entries can be long and tedious. One can properly utilize the structural symmetry to reduce the times of matrix

multiplication. The simultaneous conditions for solving S_i and T_i are established by matching coefficients of the $\cos^n \theta$ term of the IL function with those of Chebyshev polynomial, as shown above. We derive the IL functions for such filters of order $N \leq 5$.

The results are

$$\frac{P_o}{P_L} = 1 + \left[\frac{\cos \theta_m S_1 (S_1^2 - T_1^2)}{2T_1^2 \sin \theta} \right]^2 [\mathbf{T}_1(x)]^2 \quad (4.9)$$

when $N = 1$, and

$$\frac{P_o}{P_L} = 1 + \left[\frac{1}{2T_1 T_2 \dots T_{N+1} k \sin \theta} \right]^2 [\mathbf{T}_N(x)]^2 \quad (4.10)$$

when $N = 2 \sim 5$. The simultaneous conditions for determining S_i and T_i are listed in Table 4.1. It is found that $S_1 = 2$ for each N . Note that total number of S_i and T_i for an N -order filter is $N+1$ for odd N and $N+2$ for even N . The number of conditions, including the specified ripple level, is less than that of unknowns, when $N \geq 4$. In addition, the variable k introduces an extra degree of freedom in the coefficient matching. Thus, the total degrees of freedom for $N \leq 5$ are $[N/2]$, where $[N/2]$ is an integer by truncating $N/2$. This under-determined feature is very helpful for circuit realization. This will be addressed in Section 4-3.

TABLE 4.1
THE CHEBYSHEV CONDITIONS FOR $N = 1 \sim 5$.

N	Chebyshev Conditions	Degree of Freedom
1	$S_1 = 2$	0
2	$S_1 = 2$ $2T_2^2 - T_1^4 / 2 = 1/k$ $(S_1 + S_2)[S_1 T_1^2 - 2(S_1 + S_2)] = -2/(k \cos^2 \theta_m)$	1
3	$S_1 = 2$ $4T_2^2(S_1 + S_2) - T_1^2(S_1 T_2^2 + S_2 T_1^2) = 3/(k \cos \theta_m)$ $S_2(S_1 + S_2)[S_1 T_1^2 - 2(S_1 + S_2)] = -2/(k \cos^3 \theta_m)$	1
4	$S_1 = 2$ $2T_2^4 - T_1^4 T_3^2 / 2 = 1/k$ $2T_3^2(S_1 + S_2)^2 + (S_1 + S_2)[4T_2^2(S_2 + S_3) - S_1 T_1^2 T_3^2] - [S_1 T_2^2 + T_1^2(S_2 + S_3)]^2 / 2 + 2T_2^4 = 8/(k \cos^2 \theta_m)$ $(S_1 + S_2)(S_2 + S_3)^2 [S_1 T_1^2 - 2(S_1 + S_2)] = -8/(k \cos^4 \theta_m)$	2
5	$S_1 = 2$ $T_2^2 T_3^2 [S_1 T_1^2 - 4(S_1 + S_2)] + T_1^4 T_3^2 (S_2 + S_3) - 4S_3 T_2^4 = -5/k \cos \theta_m$ $(S_2 + S_3)\{2(S_1 + S_2)[4S_3 T_2^2 - S_1 T_1^2 T_3^2 + 2T_3^2(S_1 + S_2)] - S_3 T_1^4 (S_2 + S_3) - 2S_1 S_3 T_1^2 T_2^2\} = 20/(k \cos^3 \theta_m)$ $S_3(S_1 + S_2)(S_2 + S_3)^2 [S_1 T_1^2 - 2(S_1 + S_2)] = -8/(k \cos^5 \theta_m)$	2

4-2 The Ripple Level and Bandwidth

The $1/\sin\theta$ term in (4.10) will alter the specified ripple level R to a certain extent. When $N \leq 3$, a method for correcting R will be formulated. For $N \geq 4$, the $1/\sin\theta$ term also deviates the uniformity of passband ripples slightly. A strategy for its improvement will be investigated.

4-2-1 Ripple Level Specified by θ_m :

Take the second-order filter as an example again. The passband ripple level can be obtained by evaluating the IL function (4.8) at $\theta = \theta_m$, edges of the passband, i.e.,

$$R \text{ (dB)} = 10 \log \left\{ 1 + \left[\frac{1}{2T_1^2 T_2 k \sin \theta_m} \right]^2 \right\} \quad (4.11)$$

It can be rewritten as

$$T_1^2 T_2 = \frac{1}{2k \sin \theta_m \sqrt{10^{\frac{R}{10}} - 1}} \quad (4.12)$$

This is called the ripple level condition herein. Based on (4.7a) ~ (4.7c) and (4.12), the variables S_1 , S_2 , T_1 , and T_2 can be solved. For example, if $R = 3\text{dB}$ and fractional bandwidth $\Delta = 50\%$, the solutions are $S_1 = 2$, $T_1 = 0.83$, $S_2 = 0.981$ and $T_2 = 0.787$ with $k = 1$.

The dashed curves denoted by θ_m in Fig. 4.1 are the calculated Chebyshev response (4.8) for a filter with center frequency $f_o = 5.8\text{ GHz}$. Detailed passband in the inserted frame shows that Δ is accurately obtained, but the ripple level is 0.3dB less

than the specification. A further study shows that if a ripple level of 0.1dB is given, the decrement is about 0.01dB.

4-2-2 Ripple level specified by θ_d :

If a little BW decrement is acceptable, the decrement of R can be recovered. Let $\theta = \theta_d$ be the frequencies where peak ripples occur. Thus, the positions of θ_d can be found by

$$\frac{d}{dx}[\mathbf{T}_N(x)] = 0 \quad (4.13)$$

When $N = 2$, it leads to $x = \cos \theta_d / \cos \theta_m = 0$ or $\theta_d = \pi/2$. Enforcing the specified ripple level R at $\theta = \theta_d$, the ripple level condition (4.12) becomes

$$T_1^2 T_2 = \frac{1}{2k \sqrt{10^{\frac{R}{10}} - 1}} \quad (4.14)$$

The solid curve in Fig. 4.1 shows the calculated Chebyshev responses based on (4.14). Given $R = 3\text{dB}$ and $\Delta = 50\%$, the calculated ripple level is exactly 3 dB as expected. It is worth mentioning that the new solutions are $S_1 = 2$, $T_1 = 0.803$, $S_2 = 0.955$ and $T_2 = 0.777$ for $k = 1$, and that the new response has $\Delta = 49.7\%$, a little bit smaller than the specification.

When $N = 3$, there are two symmetric peak ripples locating on both sides of the center frequency. Fig. 4.2(a) investigates the influence of θ_d formulation on the

calculated BWs for $R = 0.5\text{dB}$. Detailed data show that when $\Delta = 30\%$, 40% , 50% , and 60% , the calculated BWs are 29.93% , 39.77% , 49.70% and 59.42% , respectively. Further studies for designed bandwidth $\Delta = 50\%$, the θ_d formulation gives $\Delta = 49.7\%$ for R varying from 0.1 to 3dB as shown in Fig. 4.2(b). Table 4.2 summarizes the results of Fig. 4.2(a) and 4.2(b). The results imply that the BW decrement will be increased as the designed BW increases, but it seems irrelative to the given ripple level. In addition, when $N \leq 5$, it is found that the BW decrements are more or less the same for filters with different orders.

When $N = 4$ and 5 , there are 3 and 4 symmetric peak ripples, respectively, locating in the passband. Thus, both cases have two ripple levels deviating from the given specification, again, due to the $1/\sin\theta$ term in (4.10).

When $N = 4$, the three $1/|S_{21}|$ peaks locate at $x = 0, \pm 0.707$ or $\theta_d = \pi/2, \pm \cos^{-1}(0.707 \times \cos\theta_m)$, obtained by enforcing the first derivative of $T_4(x)$ to zero. If $\theta_d = \pi/2$, or $f = f_o$, is chosen to locate the assigned ripple level, the other two peak levels will exceed the specification slightly. On the other hand, if $\theta_d = \pm \cos^{-1}(0.707 \times \cos\theta_m)$ are used, the central peak ripple will be slightly less than specification. This θ_d will be preferred since the given ripple level defines the maximal in-band ripple level. Fig. 4.3 shows the detailed $|S_{21}|$ responses of fourth-order filters based on the θ_d formulation for $\Delta = 50\%$ and $R = 0.1, 0.5, \text{ and } 1\text{ dB}$. When $R = 1\text{ dB}$, the central peak ripple level is 0.93dB , only 0.07dB away from the design. When R is small, the ripple level decrements seem to be negligible.

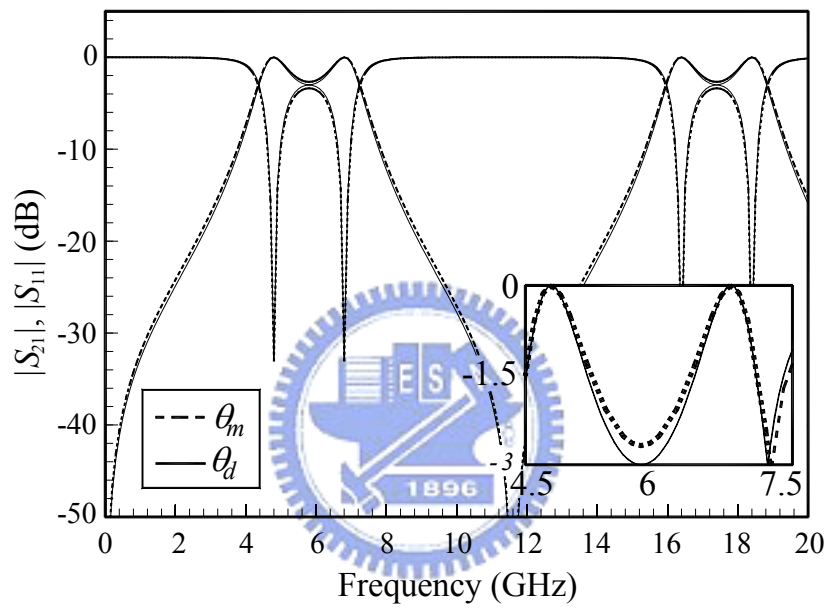
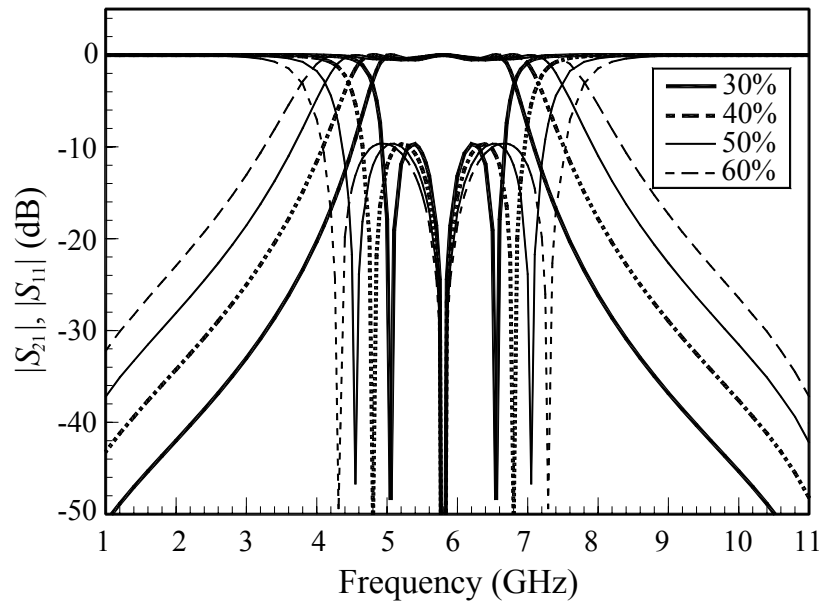
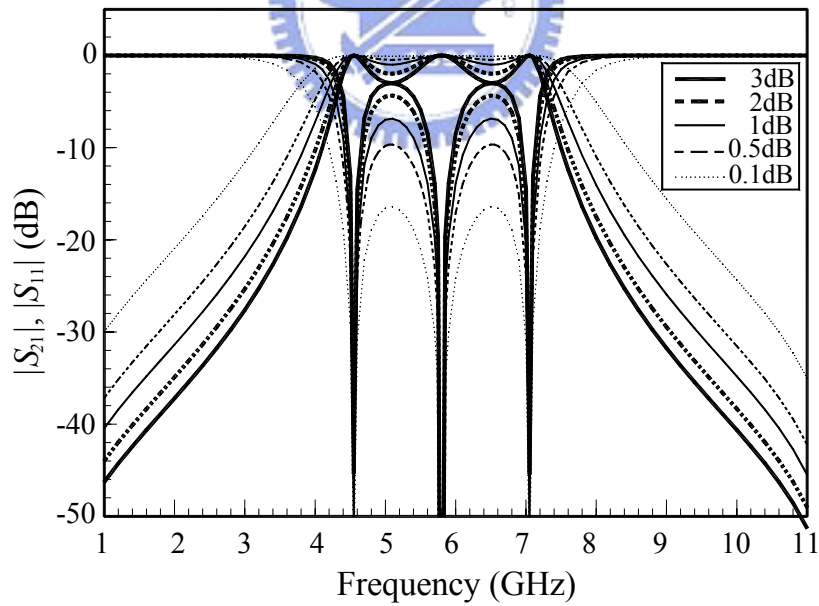


Fig. 4.1 Calculated Chebyshev responses with ripple levels specified by θ_m and θ_d . $N = 2$, $R = 3$ dB, $\Delta = 50\%$, $f_o = 5.8$ GHz.



(a)



(b)

Fig. 4.2 Calculated responses of third-order Chebyshev filters, with ripple levels specified by θ_a . (a) With ripple level $R = 0.5\text{dB}$. (b) With designed bandwidth $\Delta = 50\%$.

TABLE 4.2

THE INFLUENCES OF USING θ_i ON RIPPLE LEVEL DESIGN OF THIRD-ORDER FILTERS

Given ripple level = 0.5dB					
Given bandwidth (%)	30	40	50	60	
Calculated bandwidth with <i>IL</i> function (%)	29.93	39.77	49.7	59.42	
Given bandwidth = 50%					
Given ripple level (dB)	0.1	0.5	1	2	3
Calculated bandwidth with <i>IL</i> function (%)	49.7	49.7	49.7	49.7	49.7

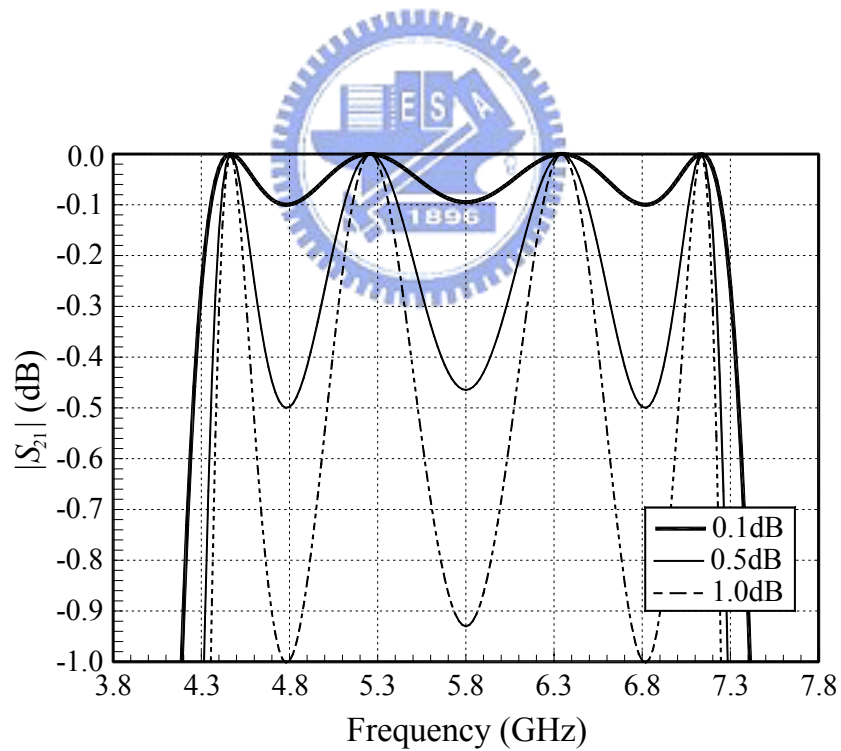


Fig. 4.3 Detailed $|S_{21}|$ performance within passband of fourth-order filters with ripple levels specified by θ_i . $\Delta = 50\%$, $R = 0.1, 0.5$ and 1dB .

4-3 Three Examples

Three filters are synthesized and fabricated at $f_o = 5.8$ GHz for demonstration. A third-order filter η is designed with $\Delta = 50\%$ and $R = 0.5$ dB, a fourth-order filter ξ and a fifth-order filter ψ are synthesized with $\Delta = 40\%$ and $R = 0.1$ dB. The full-wave EM software package IE3D [10] is used for circuit simulation. The θ_d formulation is used for defining the maximal in-band ripple level.

4-3-1 Filter η ($N = 3$, $\Delta = 50\%$, $R = 0.5$ dB):

When $N = 3$, four geometric variables have to be solved for two of four coupled stages. With $\theta_d = \cos^{-1}(\cos \theta_m/2)$, the ripple level condition becomes

$$T_1 T_2 = \frac{1}{\sqrt{2k \sin(\cos^{-1}(\cos \theta_m/2))} \sqrt{10^{\frac{R}{10}} - 1}} \quad (4.15)$$

From (4.5c), we have $\theta_m = 1.1781$ rad, and hence $\theta_d = 1.3783$ rad. Based on the three conditions listed in Table 4.1 and (4.15), possible roots for T_1 , S_2 and T_2 with respect to k ranging from 0.3 to 2.0 are plotted in Fig. 4.4. Obviously, not all roots shown in Fig. 4.4 are practical using the standard microstrip technology. Note that geometry of coupled stage i will be determined by $Z_{oei} = (S_i + T_i) \times Z_o/2$ and $Z_{ooi} = (S_i - T_i) \times Z_o/2$, with Z_o being the system impedance. Suppose that the circuit substrate has $\epsilon_r = 10.2$ and thickness $d = 1.27$ mm. Our fabrication facilities require both G/d and W/d no less than 0.1. When $Z_o = 50 \Omega$, solutions of Z_{oe} and Z_{oo} for the first and second stages are plotted together with the design graph in Fig. 4.5, which is very useful for seeking adequate roots from realization point of view. As k is increased, values of Z_{oo1} increases

while those of Z_{oe1} , Z_{oe2} and Z_{oo2} decrease. As shown in Fig. 4.5, there is no possible solution to the first stage. The tapped structure in Chapter 3 can be used to replace the end stage with a $\lambda/4$ line with characteristic impedance $Z_1 = (Z_{oe} - Z_{oo})/2$ and tap point being at the outer open end. Fig. 4.6 investigates the performance of the equivalence. Three coupled stages with $(Z_{oe}, Z_{oo}) = (86 \Omega, 14 \Omega)$, $(86.08 \Omega, 13.92 \Omega)$ and $(86.5 \Omega, 13.5 \Omega)$ for using in the three experimental filters are studied. All of them have a maximal $|S_{21}|$ deviation less than 0.13dB within a BW of 50%.

With the tapped input/output, criterion for choosing the solution becomes to release dimensions of middle stages and locate all difficulties to the end stages as much as possible. Thus, the solution is then chosen as $S_1 = 2$, $T_1 = 1.44$, $S_2 = 3.366$ and $T_2 = 1.531$ with $k = 0.3$. The corresponding modal characteristic impedances for all stages are listed in Table 4.3 with $Z_o = 50 \Omega$. The tapped resonator has $Z_1 = 36 \Omega$ for substituting the end stages with $Z_{oe1} = 86 \Omega$ and $Z_{oo1} = 14 \Omega$.

Fig. 4.7(a) plots the theoretical, simulated and measured responses. The simulated and measured results show good agreement with the theoretical response. The inserted frame shows the three detailed $|S_{21}|$ curves within the passband. Detailed data show that the fractional BWs of the simulated and measured results have only -0.5% and -1% , respectively, away from the theoretical design. In measurement, in-band IL is 0.6 dB, and ripple level is close to 0.6 dB. The 0.1 dB deviation causes a 6-dB decrement in the $|S_{11}|$ response. Photograph of the fabricated circuit is in Fig. 4.7(b).

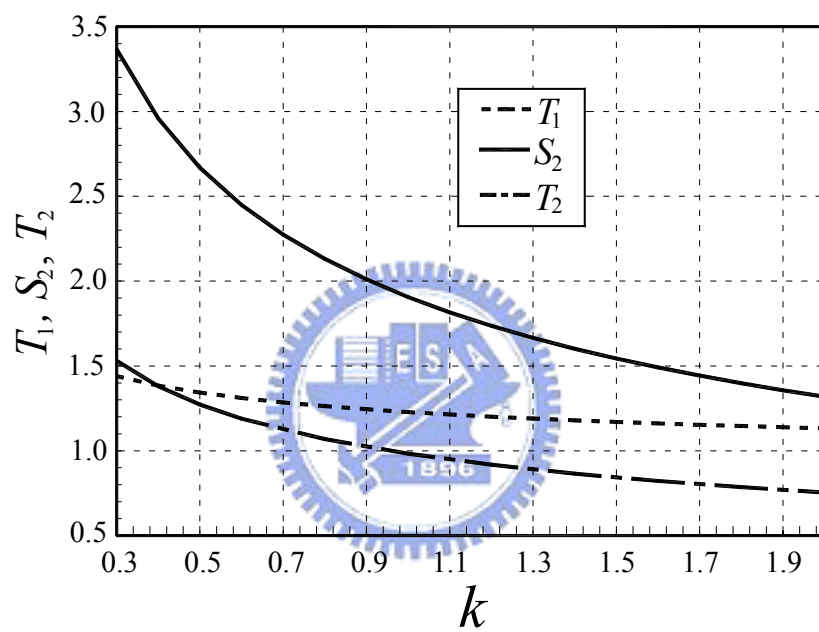


Fig. 4.4 Possible roots for T_1, S_2 and T_2 with respect to k for a third-order filter with $R = 0.5$ dB and $\Delta = 50\%$.

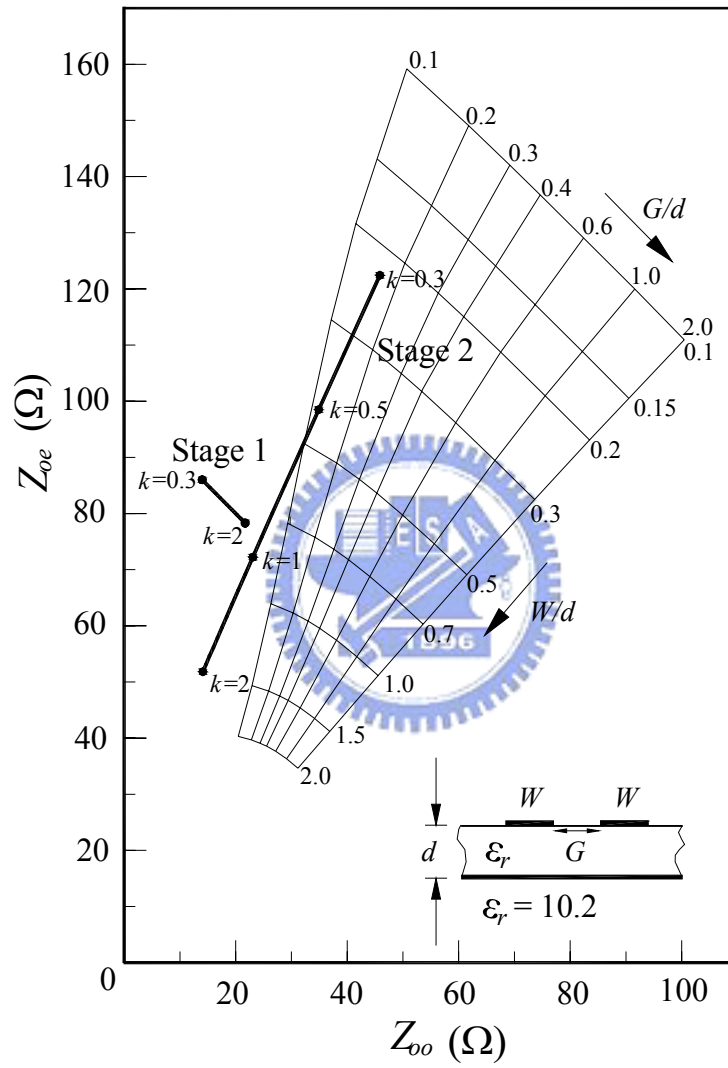


Fig. 4.5 Root loci for Z_{oe} and Z_{oo} of the first and second stages of third-order filter when $Z_o = 50 \Omega$.

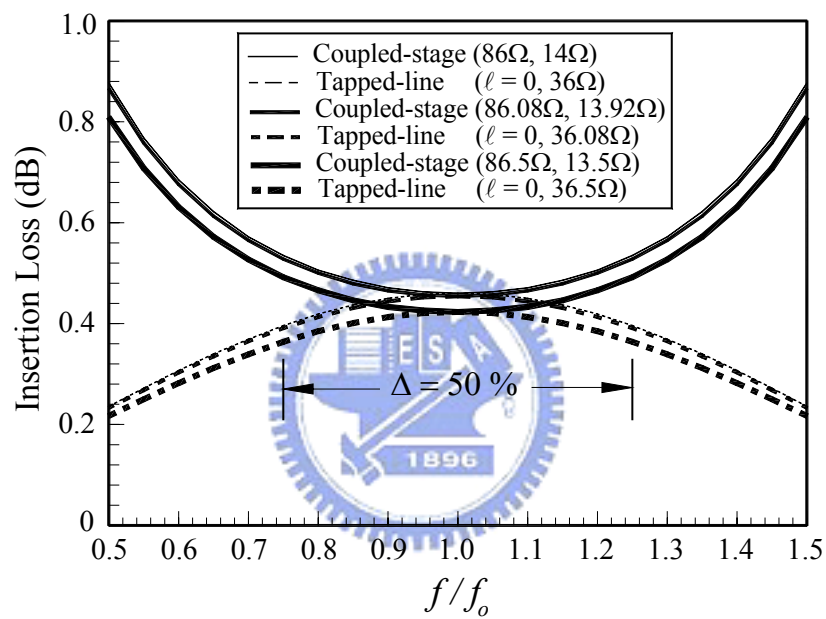
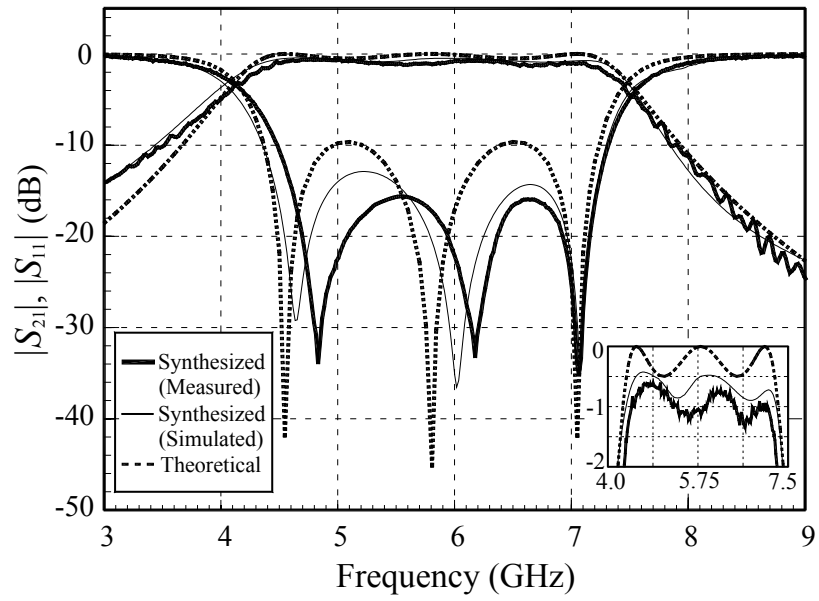
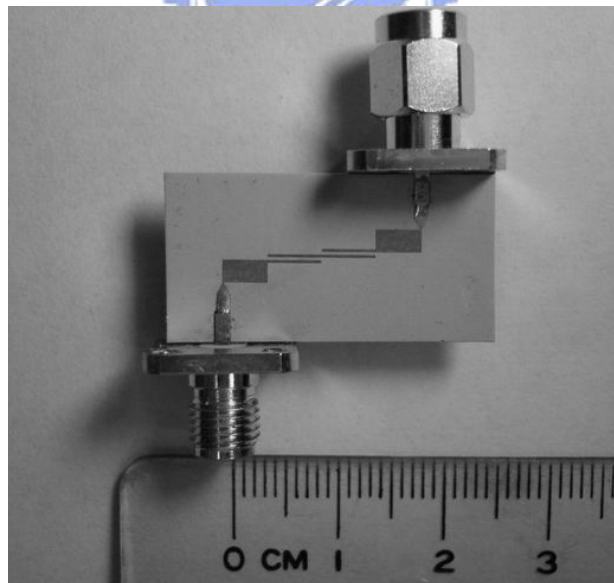


Fig. 4.6 Comparison of $|S_{21}|$ responses of tapped lines and coupled stages.



(a)



(b)

Fig. 4.7 (a) Theoretical, simulated and measured responses of filter η . (b) Photograph of the fabricated circuit. $f_o = 5.8\text{GHz}$, $N = 3$, $\Delta = 50\%$, $R = 0.5\text{dB}$. Circuit dimensions: $W_1 = 2\text{mm}$, $W_2 = 0.286\text{mm}$, $G_2 = 0.206\text{mm}$. Substrate: $\epsilon_r = 10.2$, thickness = 1.27 mm.

TABLE 4.3
THE CHOSEN ROOTS AND MODAL IMPEDANCES OF THE THREE EXPERIMENTAL FILTERS
WITH TAPPED INPUTS

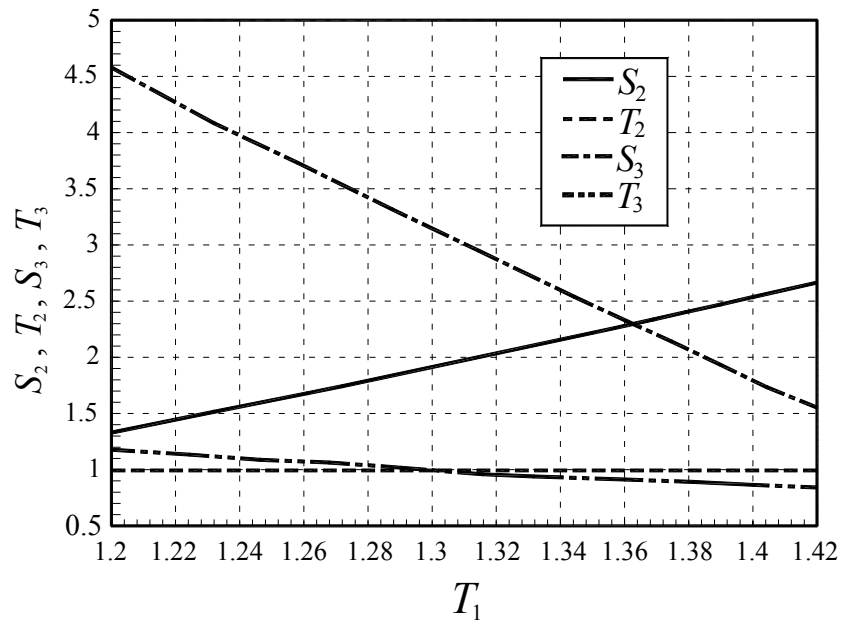
Filters	1 st stage	2 nd stage	3 rd stage
η $N = 3$ $\Delta = 50\%$ $Z_o = 50\Omega$	$S_1 = 2$ $T_1 = 1.44$ $\ell = 0$ $Z_1 = 36\Omega$	$S_2 = 3.366$ $T_2 = 1.531$ $Z_{oe2} = 122.43\Omega$ $Z_{oo2} = 45.87\Omega$	Same as the 2nd stage
ξ $N = 4$ $\Delta = 40\%$ $Z_o = 50\Omega$	$S_1 = 2$ $T_1 = 1.443$ $\ell = 0$ $Z_1 = 36.08\Omega$	$S_2 = 2.803$ $T_2 = 1.181$ $Z_{oe2} = 99.63\Omega$ $Z_{oo2} = 40.53\Omega$	$S_3 = 2.991$ $T_3 = 1.154$ $Z_{oe3} = 103.63\Omega$ $Z_{oo3} = 45.93\Omega$
ψ $N = 5$ $\Delta = 40\%$ $Z_o = 50\Omega$	$S_1 = 2$ $T_1 = 1.46$ $\ell = 0$ $Z_1 = 36.5\Omega$	$S_2 = 3.03$ $T_2 = 1.284$ $Z_{oe2} = 107.85\Omega$ $Z_{oo2} = 43.65\Omega$	$S_3 = 3.972$ $T_3 = 1.388$ $Z_{oe3} = 133.99\Omega$ $Z_{oo3} = 64.61\Omega$

4-3-2 Filter ξ ($N = 4$, $\Delta = 40\%$, $R = 0.1dB$):

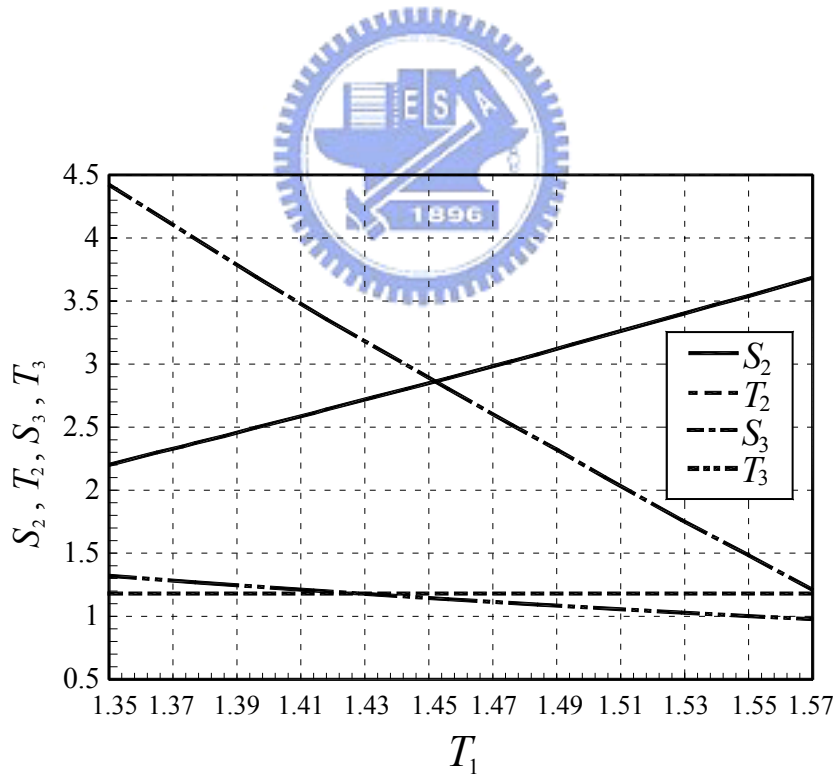
When $N = 4$, six variables have to be determined. Let $\theta_d = \cos^{-1}(0.707 \times \cos \theta_m)$, then the ripple level condition can be derived as

$$T_1^2 T_2^2 T_3 = \frac{1}{2k \sin(\cos^{-1}(0.707 \times \cos \theta_m)) \sqrt{10^{\frac{R}{10}} - 1}} \quad (4.16)$$

Two free dimensions exist for this design. One is from that six variables are specified by (4.16) and the four Chebyshev conditions in Table 4.1 and the other from k . Since $\Delta = 40\%$, $\theta_m = 1.2566$ rad. We can take k and T_1 as sweep variables to solve the simultaneous equations. The possible solutions for S_2 , T_2 , S_3 and T_3 with respect to T_1 are shown in Fig. 4.8(a) ~ 4.8(c) with $k = 2, 1$ and 0.5 , respectively. Observe that the values of S_3 and T_3 drop off with T_1 , while S_2 increases oppositely. The value of T_2 only varies with k . For each T_1 , Z_{oei}/Z_o is average of the two curves of S_i and T_i , and Z_{ooi}/Z_o is half the distance between them. For implementation, the larger value of S_i and larger distance between S_i and T_i are preferred. Since there are different tendencies for second and third stages, compromises must be made in choosing roots. Fig. 4.9 plots the root loci for Z_{oo} and Z_{oe} of the second and third stages when $Z_o = 50 \Omega$ and $k = 0.5, 1$, and 2 . The root loci indicate that most of solutions fall into the fan area of $G/d \geq 0.1$ and $W/d \geq 0.1$. We choose a solution with $k = 1$ for demonstration. Each end stage with $Z_{oe1} = 86.08 \Omega$ and $Z_{oo1} = 13.92 \Omega$ is replaced by a tapped section with $Z_1 = 36.08 \Omega$. As shown in Fig. 4.10(a), the simulated and measured results match very well with the theoretical prediction. Detailed data show that both simulated and measured responses have BWs of 39.1% and 39.3%, respectively. The circuit photograph is in Fig. 4.10(b).



(a)



(b)

Fig. 4.8. Possible roots for S_2 , T_2 , S_3 and T_3 with respect to T_1 for a fourth-order filter with $R = 0.1\text{dB}$ and $\Delta = 40\%$. (a) With $k = 2$. (b) With $k = 1$. (c) With $k = 0.5$.

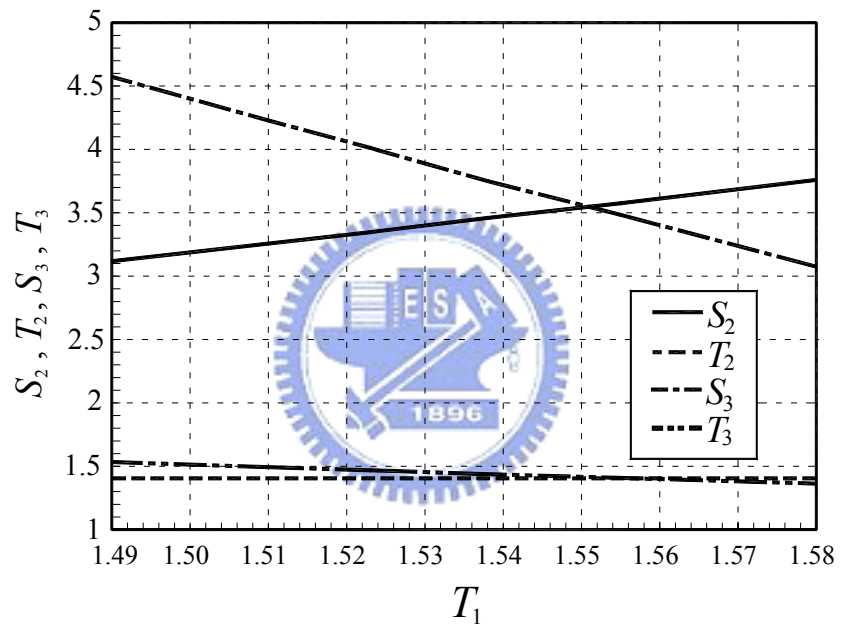


Fig. 4.8(c)

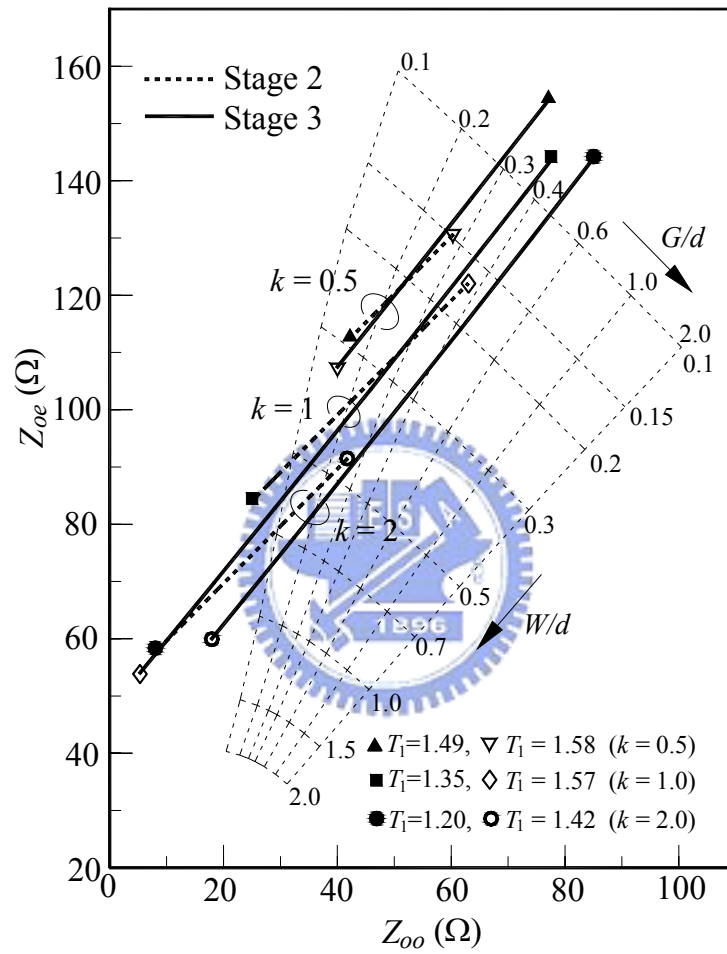
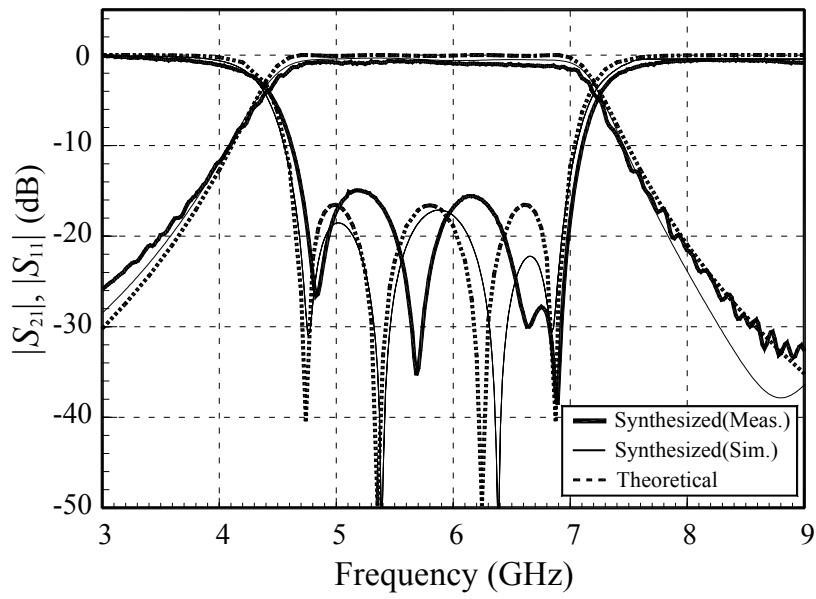
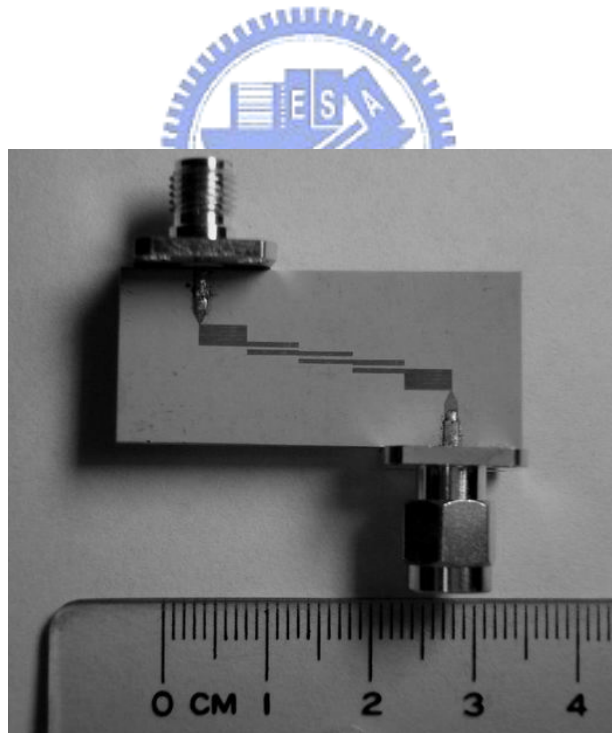


Fig. 4.9 Root loci for Z_{oe} and Z_{oo} of the second and third stages of a fourth-order Chebyshev filter with $k = 2, 1$ and 0.5 when $Z_o = 50 \Omega$.



(a)



(b)

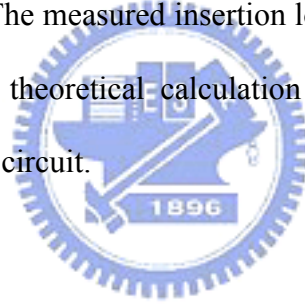
Fig. 4.10 (a) Theoretical, simulated and measured responses of filter ξ , $f_o = 5.8\text{GHz}$, $N = 4$, $\Delta = 40\%$, $R = 0.1\text{dB}$. (b) Photograph of the fabricated circuit. Circuit dimensions: $W_1 = 2\text{mm}$, $W_2 = 0.49\text{mm}$, $W_3 = 0.41\text{mm}$, $G_2 = 0.23\text{mm}$, $G_3 = 0.31\text{mm}$.

4-3-3 Filter ψ ($N=5$, $\Delta = 40\%$, $R = 0.1\text{dB}$):

The third experiment is a fifth-order filter with $\Delta = 40\%$ and $R = 0.1\text{dB}$. From $d/dx(\mathbf{T}_5(x)) = 0$, we have $\theta_d = \cos^{-1}(0.809 \times \cos \theta_m)$. The ripple level condition is

$$T_1 T_2 T_3 = \frac{1}{\sqrt{2k \sin(\cos^{-1}(0.809 \times \cos \theta_m))} \sqrt{10^{\frac{R}{10}} - 1}} \quad (4.17)$$

Fig. 4.11 plots the filtered roots with $\theta_m = 1.2566$ radian, $R = 0.1\text{dB}$ and $k = 0.5$. Fig. 4.12(a) plots theoretical, simulation and measured results. The end stages, with $Z_{oe1} = 86.5 \Omega$ and $Z_{oo1} = 13.5 \Omega$, are replaced by tapped $\lambda/4$ sections with $Z_1 = 36.5\Omega$. All of them show good agreement. The measured insertion loss is 0.7dB. The measured BW is about 1.9% less than the theoretical calculation by (4.10). Fig. 4.12(b) is the photograph of the experiment circuit.



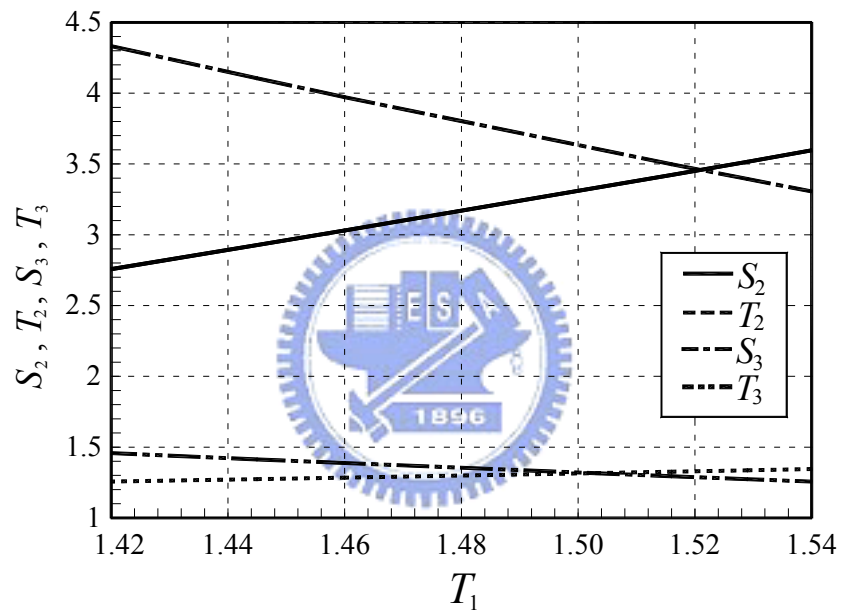
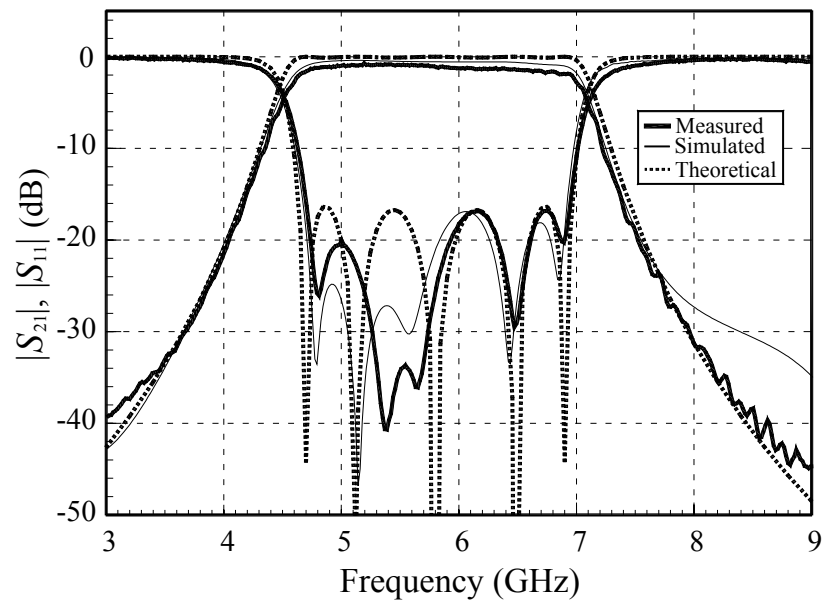
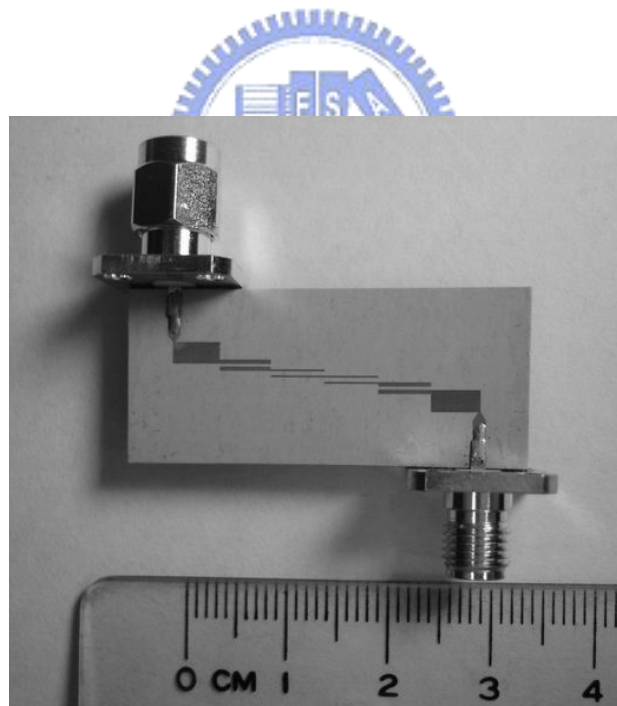


Fig. 4.11 Possible roots for the 2nd and 3rd coupled stages of a fifth-order parallel-coupled line filter with $\Delta = 40\%$, $R = 0.1\text{dB}$ and $k = 0.5$.



(a)



(b)

Fig. 4.12 (a) Theoretical, simulated and measured responses of filter $\psi, f_o = 5.8\text{GHz}, N = 5, \Delta = 40\%, R = 0.1\text{dB}$. (b) Photograph of the fabricated circuit. Circuit dimensions: $W_1 = 1.97\text{mm}, W_2 = 0.4\text{mm}, W_3 = 0.16\text{mm}, G_2 = 0.25\text{mm}, G_3 = 0.39\text{mm}$.

Chapter 5

Conclusion

For recovering the BW decrement, new formulas for determining Z_{oe} and Z_{oo} of each coupled stage have been derived in Chapter 2 for synthesizing relatively wideband filters. A third- and a fifth-order Chebyshev filters with 50% designed bandwidth are fabricated and measured. The measurements show that the proposed formulas not only provide a significant improvement in predicting the filter bandwidth, but also preserve the quality of passband responses.

As presented in Chapter 2, the realized BWs can be greatly improved, but the BW decrement is still not completely resolved. In Chapter 3, parallel coupled-line filters with maximally flat responses of order $N \leq 6$ are synthesized based on derived insertion loss functions. Simultaneous equations for maximally flat responses and the Q_T condition are formulated for determining Z_{oe} and Z_{oo} of each coupled stage. The under-determined conditions leave several degrees of freedom in choosing the circuit dimensions. By properly utilizing these degrees of freedom, the problem resulted from the tight coupled-line dimensions can be resolved by gathering all difficulties to the end stages and employing tapped input/output to replace the end stages. Five circuits are simulated and three of them are fabricated and measured to demonstrate the formulation and circuit synthesis. The measured results manifest very accurate bandwidths.

The formulation in Chapter 3, however, is limited to maximally flat responses. Chebyshev filters can have more applications than those of the maximally flat type. From Chapter 4, parallel-coupled line filters with Chebyshev responses are directly

synthesized for order $N \leq 5$ based on derived insertion loss functions. Simultaneous equations for Chebyshev responses and the ripple level condition are formulated for determining Z_{oe} and Z_{oo} of each coupled stage. The ripple level condition can be modified to recover the error of ripple level resulted from the $1/\sin\theta$ term in the canonical Chebyshev expression. When $N \geq 4$, the in-band peak ripple levels of the synthesized filters have a slight deviation from design. The deviation is negligible when the design ripple level is small. Three circuits are fabricated and measured to validate the formulation. The proposed method provides a significant improvement in predicting the filter BW and preserve quality of Chebyshev responses.



Reference

- [1] Y. C. Yoon and R. Kohno, "Optimum multi-user detection in ultra-wideband (UWB) multiple-access communication systems", in *IEEE Int. Conf. Comm.*, pp. 812-816, 2002.
- [2] D. P. Andrews and C. S. Aitchison, "Wide-band lumped-element quadrature 3-dB couplers in microstrip," *IEEE Trans. Microwave Theory Tech.*, pp. 2424-2431, Dec. 2000.
- [3] J.-T. Kuo and E. Shih, "Wideband bandpass filter design with three line microstrip structures," *IEE Proceedings - Microwaves, Antennas and Propagation*, vol.149, No.5, pp. 243-247, Oct. 2002.
- [4] L. Zhu, H. Bu and K. Wu "Broadband and compact multi-pole microstrip bandpass filters using ground plane aperture technique," *IEE Proc. - Microwaves, Antennas Propagation*, pp.71-77, Feb. 2002.
- [5] C.-Y. Chang and T. Itoh, "A modified parallel-coupled filter structure that improves the upper stopband rejection and response symmetry," *IEEE Trans. Microwave Theory Tech.*, pp. 310-314, Feb. 1991.
- [6] G. L. Matthaei, L. Young and E. M. T. Johns, *Microwave Filters, Impedance Matching Networks, and Coupling Structures*. Norwood MA: Artech House, 1980.
- [7] D. M. Pozar, *Microwave Engineering*, 2nd ed., New York: John Wiley & Sons, 1998.
- [8] J. M. Drozd and W. T. Joines, "Maximally flat quarter-wavelength- coupled transmission-line filters using Q distribution," *IEEE Trans. Microwave Theory Tech.*, vol. 45, pp.2100-2113, Dec. 1997.
- [9] R. Levy, "Theory of Direct Coupled Cavity Filters," *IEEE Trans. Microwave Theory Tech.*, pp.340-348, June 1967.
- [10] Zeland Software Inc., *IE3D simulator*, Jan. 1997.
- [11] S. B. Cohn, "Parallel-coupled transmission-line resonator filters," *IRE Trans. Microwave Theory Tech.*, vol. MTT-6, pp.223~231, Apr. 1958.

- [12] L. Zhu, W. Menzel, K. Wu, and F. Boegelsack "Theoretical characterization and experimental verification of a novel compact broadband microstrip bandpass filter," *Proc. of APMC2001*, pp.625-628, 2001.
- [13] K.-S. Chin, L.-Y. Lin and J.-T. Kuo, "New formulas for synthesizing microstrip bandpass filters with relatively wide bandwidths," *IEEE Trans. Microwave and Wireless Components Letters*, vol.14, pp. 231-233, May 2004.
- [14] W. W. Mumford, "Tables of stub admittances for maximally flat filters using shorted quarter-wave stubs," *IEEE Trans. Microwave Theory Tech.*, vol. MTT-13, pp.695~696, Sept. 1965.
- [15] E. G. Cristal, "Tapped-line coupled transmission lines with applications to interdigital and combline filters," *IEEE Trans. Microwave Theory Tech.*, vol. MTT-23, pp.1007-1012, Dec. 1975.
- [16] J. S. Wong, "Microstrip tapped-line filter design," *IEEE Trans. Microwave Theory Tech.*, vol. MTT-27, pp.44-50, Jan. 1979.
- [17] K.-S. Chin and J.-T. Kuo, "Insertion loss function synthesis of maximally flat parallel-coupled line bandpass filters," accepted for publication in the *IEEE Trans. Microwave Theory Tech.* (Sept. Issue of the 2005 IEEE MTT)
- [18] K.-S. Chin and J.-T. Kuo, "Direct synthesis of parallel-coupled line bandpass filters with Chebyshev responses," submitted to *IEEE Trans. Microwave Theory Tech.*, May 2005.
- [19] K.-S. Chin, L.-Y. Lin and J.-T. Kuo, "An improved formula for design of wideband parallel-coupled microstrip bandpass filters," in the *Proceedings of 2003 Progress in Electromagnetics Research Symposium (PIERS)*, pp.72, Hawaii.
- [20] K.-S. Chin and J.-T. Kuo, "Maximally flat parallel-coupled line filters using insertion loss function," accepted for publication in *2005 Cross Strait Tri-regional Radio Science and Wireless Technology Conference*, 2005
- [21] R. Levy, "New equivalent circuits for inhomogeneous coupled lines with synthesis applications," *IEEE Trans. Microwave Theory Tech.*, vol. 36, No. 6, pp.1087~1094, June 1988.

- [22] R. Levy, "Tables of element values for the distributed low-pass prototype filter," *IEEE Trans. Microwave Theory Tech.*, vol. MTT-13, pp.514~536, Sep. 1965
- [23] L. Young, "Direct-coupled cavity filters for wide and narrow bandwidths," *IEEE Trans. Microwave Theory Tech.*, vol. MTT-11, pp.162~178, May 1963.
- [24] M. Makimoto and S. Yamashita, "Bandpass filters using parallel-coupled stripline stepped impedance resonators," *IEEE Trans. Microwave Theory Tech.*, MTT-28, No.12, pp.1413-1417, Dec. 1980.
- [25] K. Wada and O. Hashimoto, "Fundamentals of open-ended resonators and their application to microwave filters," *IEICE Trans. Electron*, vol. E83-C, No.11, pp. 1763-1775, Nov. 2000.
- [26] J.-T. Kuo and E. Shih, "Microstrip stepped impedance resonator bandpass filter with an extended optimal rejection bandwidth," *IEEE Trans. Microwave Theory Tech.*, vol. 51, pp. 1554-1559, May. 2003.
- [27] W. W. Mumford, "Maximally flat filters in waveguide," *Bell Syst. Tech. J.*, vol. 27, pp. 684~713, Oct. 1948.
- [28] D. Ahn, C.-S. Kim, M.-H. Chung, D.-H. Lee, D.-W. Lew, and H.-J. Hong, "The design of parallel coupled line filter with arbitrary image impedance", in the *IEEE MTT-S Symp. Digest*, pp. 909-912, 1998.
- [29] S. L. March, "Phase velocity compensation in parallel-coupled microstrip", in the *IEEE MTT-S Symp. Digest*, pp. 410-412, 1982.
- [30] W. T. Joines and J. R. Griffin, "On using the Q of transmission lines," *IEEE Trans. Microwave Theory Tech.*, vol. MTT-16, pp. 258-260, Apr. 1968.
- [31] J. R. Griffin and W. T. Joines, "The general transfer matrix for networks with open-circuited or short-circuited stubs," *IEEE Trans. Circuit Theory*, vol. CT-16, pp. 373-376, Aug. 1969.
- [32] H. J. Riblet, "General synthesis of quarter-wave impedance transformers," *IRE Trans. Microwave Theory Tech.*, vol. MTT-5, pp. 36-43, Jan. 1957.
- [33] R. A. Dell-Imagine, "A parallel-coupled microstrip filter design procedure," in the *GMTT Symp. Digest*, pp. 29-32, 1970.
- [34] K. Whiting, "The effect of increased design bandwidth upon

- directed-coupled-resonator filters,” *IEEE Trans. Microwave Theory Tech.* (Correspondence), vol. MTT-11, pp. 557-560, Nov. 1963.
- [35] B. Easter and C. Gupta, “More accurate model of the coupled microstripline section,” *Microwave, Optics and Acoustics*, vol. 3, No. 3, pp. 99-103, May 1979.
- [36] B. Easter and K. A. Merza, “Parallel-coupled-line filters for inverted-microstrip and suspended-substrate MIC’s,” *11th European Microwave Conf. Proc.*, pp. 164-168, 1981.
- [37] I. E. Lösch and Johannes A. G. Malherbe, “Design procedure for inhomogeneous coupled line sections,” *IEEE Trans. Microwave Theory Tech.*, vol. 36, No. 7, pp. 1186-1190, July 1988.
- [38] G. L. Matthaei, “Design of wide-band (and narrow-band) band-pass microwave filters on the insertion loss basis,” *IRE Trans. Microwave Theory Tech.*, vol. MTT-8, pp. 580-593, Nov. 1960.
- [39] E. G. Cristal, “New design equations for a class of microwave filters,” *IEEE Trans. Microwave Theory Tech.*, vol. MTT-19, pp. 486-490, May 1971.
- [40] W. W. Mumford, “An exact design technique for a type of maximally-flat quarter-wave-coupled band pass filter,” in the *PTG/MTT National Symp. Digest*, vol. 63, pp.57~62, May 1963.

博士候選人資料

姓 名：金國生

性 別：男

出生年月日：民國 52 年 10 月 19 日

籍 貫：高雄縣鳳山市五甲一路 150 巷 2 號

學 歷：中正理工學院電機系畢業(71 年 8 月 ~ 75 年 7 月)
美國雪城大學電機研究所畢業(81 年 8 月 ~ 82 年 8 月)
國立交通大學電信工程研究所博士班(90 年 9 月 ~)

經 歷：中山科學研究院研究助理(75 年 7 月 ~ 82 年 7 月)
中山科學研究院助理研究員(82 年 8 月 ~ 92 年 3 月)
中山科學研究院副研究員(92 年 4 月 ~)

論文題目：具精確頻寬之平行耦合微帶線帶通濾波器合成方法

Publication List

Kuo-Sheng Chin

A. Journal:

- [1] **Kuo-Sheng Chin**, Liu-Yang Lin and Jen-Tsai Kuo, "New formulas for synthesizing microstrip bandpass filters with relative wide bandwidths," *IEEE Microwave and Wireless Components Letters*, vol. 14, No. 5, pp. 231-233, May 2004.
- [2] **Kuo-Sheng Chin** and Jen-Tsai Kuo, "Insertion loss function synthesis of maximally flat parallel-coupled line bandpass filters," accepted for publication in the *IEEE Trans. Microwave Theory Tech.* (Sept. Issue of the 2005 IEEE MTT)
- [3] **Kuo-Sheng Chin** and Jen-Tsai Kuo, "Direct synthesis of parallel-coupled line bandpass filters with Chebyshev responses," submitted to *IEEE Trans. Microwave Theory Tech.*, May 2005.



B. Conference:

- [1] **Kuo-Sheng Chin**, Liu-Yang Lin and Jen-Tsai Kuo, "An improved formula for design of wideband parallel-coupled microstrip bandpass filters," in the *Proceedings of 2003 Progress in Electromagnetics Research Symposium (PIERS)*, pp.72, Hawaii.
- [2] **Kuo-Sheng Chin** and Jen-Tsai Kuo, "A simple technique for measuring frequencies of a single-shot microwave pulse," presented in *Asia-Pacific Microwave Conference (APMC)*, New Delhi, India, pp. C/139, Dec. 15-18, 2004.
- [3] **Kuo-Sheng Chin** and Jen-Tsai Kuo, "Maximally flat parallel-coupled line filters using insertion loss function," accepted for publication in *2005 Cross Strait Tri-regional Radio Science and Wireless Technology Conference*, 2005.